water with bulk water (inner-sphere contribution). There is also a relaxation increase provided by the Gd^{3+} ion to water molecules which are diffusing close to the Gd^{3+} ion (second-sphere and outer-sphere contributions). The observed longitudinal relaxation rate $(1/T_1)_{obs}$ of the solvent water protons is known to depend on the concentration of Gd^{3+} ions according to Equation (1):

$$(1/T_1)_{obs} = (1/T_1)_d + r_1[Gd] \quad (1)$$

where $(1/T_1)_{obs}$ is the observed relaxation rate of water protons in the presence of Gd^{3+}, and $(1/T_1)_d$ is the diamagnetic relaxation rate of water protons in the absence of Gd^{3+}. The longitudinal relaxivity value, r_1, refers to the amount of increase in $1/T_1\ s^{-1}$ per millimolar concentration of agent (given as mM^{-1} Gd), and [Gd] is the millimolar concentration of Gd^{3+} ions. Therefore, a plot of $(1/T_1)_{obs}$ versus Gd^{3+} concentration would give the r_1 relaxivity as the slope, and the r_1 relaxivity, normally expressed in units of $mM^{-1}\ sec^{-1}$, reflects the ability of a Gd^{3+} complex to increase relaxation. The water proton relaxivities, r_1, of **[Gd-5]** and **[Gd-8]** were determined at 20 MHz (0.47 T), at 25 or 37 °C, and are shown in Table 1. In the absence of HSA, the r_1 relaxivities

Table 1. The r_1 relaxivity [$mM^{-1}\ s^{-1}$] (20 MHz) in PBS with 4.5% HSA or PBS.

Compound	HSA[a]		PBS[b]	
	25 °C	37 °C	25 °C	37 °C
[Gd-5]	6.34	6.06	5.80	5.35
[Gd-8]	8.76	9.51	4.11	3.87

[a] Human serum albumin (HSA) (4.5% w/v) in phosphate-buffered saline (PBS; 137 mM NaCl, 8.10 mM Na_2HPO_4, 2.68 mM KCl, 1.47 mM KH_2PO_4, pH 7.4). [b] PBS only.

of **[Gd-5]** are higher than those of **[Gd-8]** at both 25 and 37 °C. However, in PBS with 4.5% w/v HSA at 25 °C, the r_1 relaxivity of **[Gd-8]** is higher than that of **[Gd-5]** by 38% as a consequence of a higher albumin binding affinity; at 37 °C, where the exchange of Gd^{3+}-bound water molecules is more facile, the r_1 relaxivity of **[Gd-8]** is higher than that of **[Gd-5]** by 57%. From these results, it was considered that the increase of the $1/T_1$ value of **[Gd-5]** in Figure 2 was a consequence of enzymatic cleavage of the galactopyranose residue of **[Gd-5]** by the β-galactosidase activity. Moreover, the r_1 relaxivity of **[Gd-5]** at 20 MHz showed similar values in the absence and the presence of HSA, indicating that **[Gd-5]** hardly interacts with HSA.

Albumin binding study: We investigated the noncovalent interaction between **[Gd-5]** or **[Gd-8]**, and HSA. To demonstrate the extent of relaxation enhancement, the E-titration is shown in Figure 4.[2,11a] The longitudinal water proton relaxation times T_1 of a 0.1 mM solution of **[Gd-5]** or **[Gd-8]** in PBS with various concentrations of HSA (0–3.35 mM (0–22.5% w/v)) were measured at 20 MHz (0.47 T), 37 °C. The results were expressed in terms of the enhancement factor ε^*, that is, the ratio of paramagnetic longitudinal relaxation

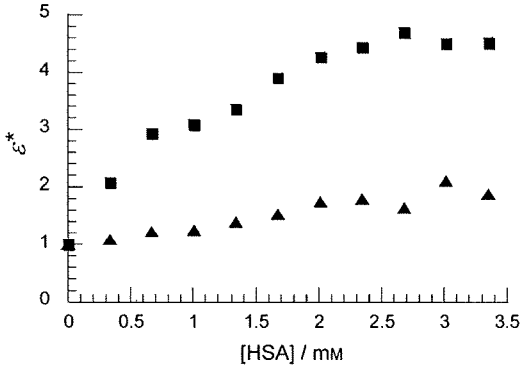

Figure 4. E-titration data for **[Gd-5]** and **[Gd-8]**. ε^* versus [human serum albumin (HSA)] in mM, at 37 °C, in phosphate-buffered saline (PBS, pH 7.4) at 20 MHz, 0.47 T. Each solution contains various concentrations of HSA (0–22.5% w/v (=0–3.35 mM) with 0.1 mM **[Gd-5]** (▲) or **[Gd-8]** (■).

rates ($(1/T_1)_{para}$ [s^{-1}]) in the presence and the absence of HSA were plotted versus increasing HSA concentration at a constant concentration of **[Gd-5]** or **[Gd-8]** (0.1 mM) [Eq. (2)]:

$$\varepsilon^* = \frac{(1/T_1)^{Alb}_{obs} - (1/T_1)^{Alb}_{dia}}{(1/T_1)^{PBS}_{obs} - (1/T_1)^{PBS}_{dia}} = \frac{(1/T_1)^{Alb}_{para}}{(1/T_1)^{PBS}_{para}} \quad (2)$$

where the *obs*, *para*, and *dia* subscripts refer to the observed, paramagnetic, and diamagnetic species, respectively, and the *Alb* and *PBS* superscripts refer to "in PBS containing human serum albumin" and "in PBS", respectively. The longitudinal water proton relaxation times T_1 of aqueous solutions without Gd^{3+} complexes were measured as the diamagnetic contribution. The longitudinal relaxation rate ($1/T_1$ [s^{-1}]) increase of **[Gd-8]** solutions in the presence of HSA was much larger than that of **[Gd-5]** solutions, and did not increase linearly with the concentration of HSA, suggesting protein binding. There was a 1.9- or 4.5-fold increase in the enhancement factor ε^* upon binding to HSA for **[Gd-5]** or **[Gd-8]**, respectively. Small parts of these increases in ε^* can be ascribed to the misleading apparent amount of water molecules (ref. [4], p. 2342). For example, ≈3 mM HSA solution contains more than 20% protein and hence less than 80% water, because of the high molecular weight of HSA. The molar concentration of 1 mmol Gd^{3+} in a liter of 20% w/v HSA is written as 1 mM, but the actual molar concentration would be 1.25 mM. However, the increase of ε^* for **[Gd-8]** is sufficiently large even when this problem is taken into consideration. Therefore, the enhancement factor ε^* for **[Gd-8]** suggests a high affinity of **[Gd-8]** for the albumin, whereas the slight increase of ε^* for **[Gd-5]** can be interpreted as indicating a weak interaction with the albumin.

Further, the binding interaction strengths of **[Gd-5]** and **[Gd-8]** to HSA were calculated by using the above E-titration experimental data.[2,11b,c,20] The observed longitudinal water proton relaxation rate, r_{1obs} [s^{-1}] is given by the sum of

three contributions, r_{1p}^{F} [$mM^{-1}s^{-1}$], r_{1p}^{B} [$mM^{-1}s^{-1}$], and r_{1dia} [s^{-1}]:

$$r_{1obs}-r_{1dia} = (r_{1P}^{F}[Gd] + r_{1p}^{B}[Gd\text{-}HSA]) \times 1000 \quad (3)$$

where r_{1p}^{F} and r_{1p}^{B} are the r_1 relaxivity [$mM^{-1}s^{-1}$] of the Gd^{3+} complex and of the paramagnetic macromolecular, Gd^{3+} complex-HSA adduct, respectively, and r_{1dia} [s^{-1}], is the diamagnetic contribution of the observed longitudinal water proton relaxation rate r_{1obs} [s^{-1}], at 20 MHz, 37 °C. [Gd], in M, is the concentration of the Gd^{3+} complex, and [Gd-HSA], in M, is the concentration of the Gd^{3+} complex-HSA adduct. The determination of the binding parameter nK_A [M^{-1}] (K_A: association constant; n: number of independent binding sites on the protein) for the equilibrium :

$$Gd + HSA \rightleftharpoons^{K_A} Gd\text{–}HSA \quad (4)$$

is possible through the following equations :

$$K_A = \frac{[Gd\text{–}HSA]}{[Gd] \cdot [n \cdot HSA]} \quad (5)$$

By combining Equations (3) and (5) we obtain Equation (6), which allows the nonlinear fitting of the experimental data :

$$r_{1obs}-r_{id} = \left(r^{F} \cdot B + (r^{B}-r^{F}) \times \frac{K_A A + K_A B + 1 - \sqrt{(K_A A + K_A B + 1)^2 - 4K_A{}^2 AB}}{2K_A} \right) \times 1000 \quad (6)$$

where A and B [both in M], are the total molar concentrations of HSA and the Gd^{3+} complex, respectively. The fitting of the experimental data into Equation (6) provided an assessment of the binding strength, nK_A [M^{-1}], and the r_1 relaxivity [$mM^{-1}s^{-1}$], of the macromolecular adduct (r_1^{B} [$mM^{-1}s^{-1}$]) (see the Supporting Information). The interaction strength of **[Gd-8]** with HSA was fairly strong ($nK_A = 7.0 \times 10^2 M^{-1}$) and the r_1 relaxivity of the paramagnetic macromolecular **[Gd-8]**-HSA adduct (r_1^{B}) was 20 $mM^{-1}s^{-1}$, at 20 MHz and 37 °C, whereas the interaction of **[Gd-5]** with HSA was rather weak ($nK_A < 1.0 \times 10^2 M^{-1}$).

Further, we examined whether various other species of albumins, such as, rat, bovine, and rabbit serum albumins, could serve as host macromolecules for **[Gd-8]**, like HSA. When **[Gd-5]** (0.1 mM) was incubated with β-galactosidase (1.13 μM), at 37 °C, for 30 min, in PBS, with 4.5% w/v human, rat, bovine, or rabbit serum albumin, all solutions showed similar decreases of the longitudinal relaxation time (T_1) of water protons (see Supporting Information).

Time-resolved luminescence and UV/Vis absorption spectra of [Tb-5] and [Tb-8]: The chemical properties of **[Gd-5]** and **[Gd-8]** were further assessed by analyzing the luminescence and chemical properties of the terbium trivalent ion (Tb^{3+}) complexes of chelator **5** and **8**, **[Tb-5]** and **[Tb-8]** (Figure 5). Lanthanide complexes, in particular complexes of Tb^{3+} and Eu^{3+} (the europium trivalent ion), have advantageous spectroscopic characteristics, such as, long luminescence lifetimes of the order of milliseconds, narrow emission peaks, a large Stoke's shift of >150 nm, and excellent water solubility.[21] This extremely long luminescence lifetime of lanthanide ions allows a time-resolved detection procedure to be employed, because typical fluorescence lifetimes are in the nanosecond region; that is, a delay time is set between the excitation pulse and the measurement of the lanthanide luminescence, during which the background fluorescence and scattered light decay to negligible levels.[22] Therefore, time-resolved luminescence measurements offer a better signal-to-noise ratio, and the lanthanide luminescence has been exploited in a number of useful detection systems for time-resolved assays in the fields of medicine, biotechnology, and biological science.[23] We prepared **[Tb-5]** and **[Tb-8]** as homologues of **[Gd-5]** and **[Gd-8]**, because the Tb^{3+} ion possesses the same charge as Gd^{3+}, as well as similar ionic radius and coordination chemistry to the Gd^{3+} ion.[24] The synthetic schemes for **[Tb-5]** and **[Tb-8]** and details of the chemical characterization of compounds are provided in the Supporting Information. As regards the metal-based luminescence properties, 25 μM aqueous solutions of **[Tb-5]** and **[Tb-8]** (in 100 mM HEPES buffer; pH 7.4) were relatively brightly luminescent upon excitation at 254 nm with a TLC plate reader lamp, and these emissions of **[Tb-5]** and **[Tb-8]** were observed with the naked eye (see Supporting Information).

First, the UV/Vis absorption spectrum of **[Tb-5]** (50 μM) and **[Tb-8]** (50 μM) was measured in 100 mM HEPES buffer at pH 7.4, 25 °C. The absorption spectra of **[Tb-5]** and **[Tb-8]** were similar, that is, **[Tb-5]** showed a λ_{max} at 279 nm tailing out to 330 nm, and **[Tb-8]** showed a λ_{max} at 281 nm tailing to 330 nm (Figure 6a). These absorption spectra can be mainly ascribed to the biphenyl substituent, because the bands observed in Tb^{3+} absorption spectra are usually very weak, that is, molar absorption coefficients (ε) of lanthanide(III) ions are usually $<1\ dm^3 mol^{-1} cm^{-1}$.[21] Second, the time-resolved luminescence spectrum of **[Tb-5]** (50 μM) or **[Tb-8]** (50 μM) was measured in 100 mM HEPES buffer (pH 7.4) upon excitation of the biphenyl substituent (excitation at 280 nm) for both **[Tb-5]** and **[Tb-8]**. The time-resolved luminescence spectra of **[Tb-5]** and **[Tb-8]**, with a delay time of 50 μs, displayed four bands (490, 545, 586, and 622 nm), arising from transitions from the emissive $^5D_4$ state to the ground-state manifolds, $^7F_6$, $^7F_5$, $^7F_4$, and $^7F_3$, respectively (Figure 6b).[21a,b] On the basis of the above spectroscopic results, the biphenyl substituent, which is the albumin-binding group, serves as a sensitizing chromophore for Tb^{3+} in the luminescent Tb^{3+} complexes, **[Tb-5]** and **[Tb-8]**.

The time-resolved luminescence spectra, with a delay time of 50 μsec, of **[Tb-5]** (50 μM) were measured in 100 mM HEPES buffer at pH 7.4, 25 °C excited at the absorbance maximum (λ_{max}) wavelength of the biphenyl group (280 nm) during the enzyme (β-galactosidase) reaction. Addition of β-

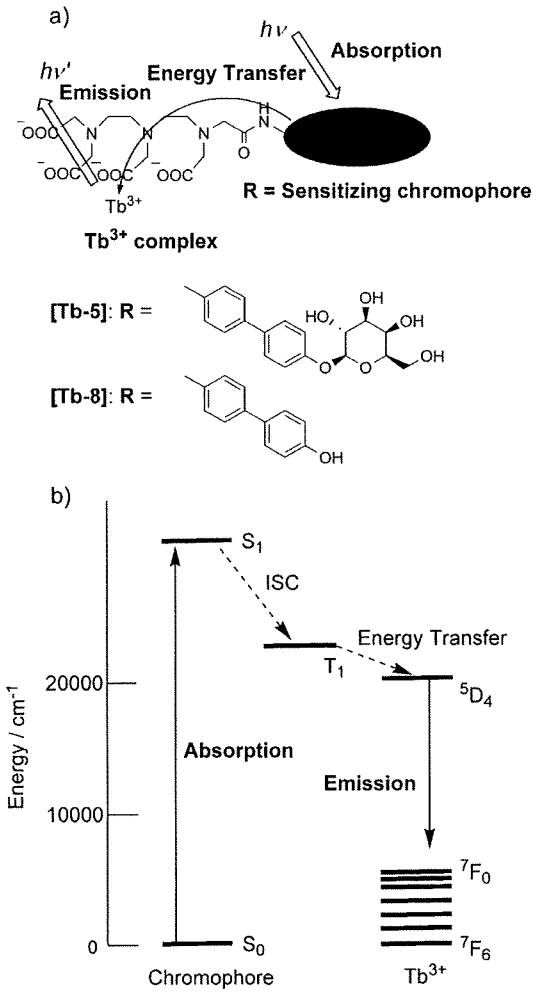

Figure 5. a) Structures of Tb^{3+} complexes, **[Tb-5]** and **[Tb-8]**, and schematic view of a chromophore incorporated into a terbium emitter. The emission from Tb^{3+} after excitation of the sensitizing chromophore on Tb^{3+} complexes, **[Tb-5]** and **[Tb-8]**, is shown. b) The general chromophore-to-terbium-ion sensitization process. Light absorption and lowest-lying singlet excited state (S_1) formation at the sensitizing chromophore are followed by intersystem crossing (ISC), resulting in population of the triplet excited state (T_1) of the sensitizing chromophore. Subsequent chromophore-to-Tb^{3+} energy transfer leads to a metal-centered emission, which is derived from transitions from Tb^{3+}-emitting states to the relevant ground states.

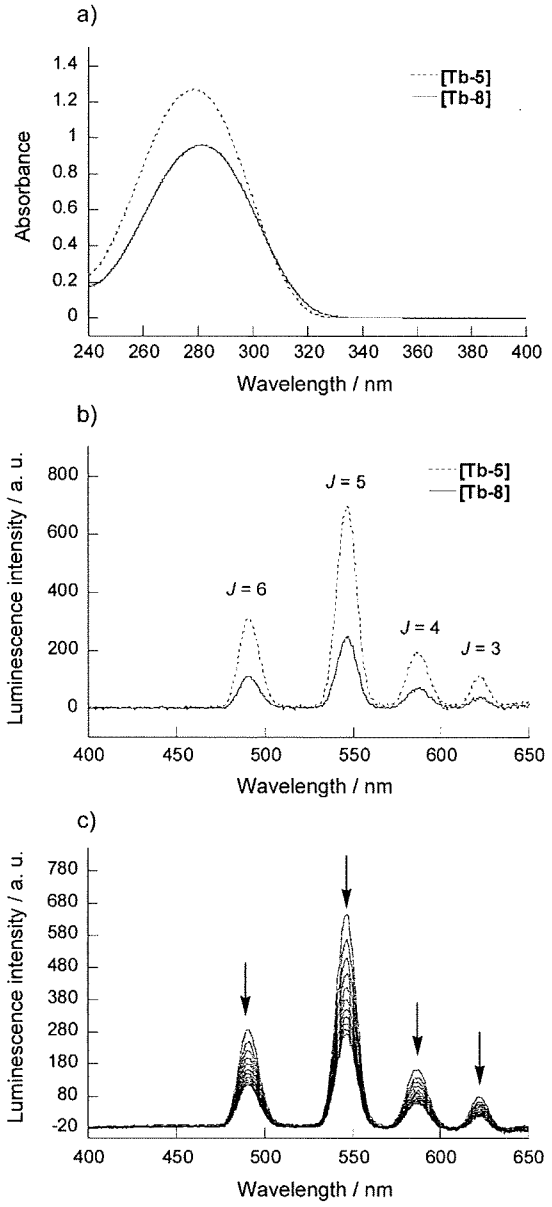

Figure 6. Spectroscopic characteristics of solutions of **[Tb-5]** and **[Tb-8]** upon addition of β-galactosidase. a) Absorbance spectra of 50 μM aqueous solution (100 mM HEPES buffer, pH 7.4) of **[Tb-5]** and **[Tb-8]** at 25 °C (**[Tb-5]**: ---, **[Tb-8]**: ——). b) Time-resolved emission spectra (excitation at 280 nm) of **[Tb-5]** and **[Tb-8]** (50 μM) (**[Tb-5]**: ---, **[Tb-8]**: ——). These spectra were measured in 100 mM HEPES buffer at pH 7.4 and 25 °C by using a delay time of 50 μs and a gate time of 1.00 ms. The bands arise from $^5D_4 \rightarrow {}^7F_J$ transitions; the J values of the bands are labeled. c) Time-resolved emission spectra (excitation at 280 nm) of **[Tb-5]** (50 μM) after the addition of β-galactosidase (113 nM) in 100 mM HEPES buffer (pH 7.4) at 25 °C. Time-resolved emission spectra of **[Tb-5]** were measured every 10 min (0≈100 min) after the addition of β-galactosidase.

galactosidase (113 nM) to an aqueous solution of **[Tb-5]** resulted in a decrease in the luminescence of Tb^{3+} as shown in Figure 6c. The luminescence intensity at 545 nm of the **[Tb-5]** solution decreased by about 43% of the initial luminescence intensity when β-galactosidase was added. HPLC monitoring of the conversion of **[Tb-5]** into **[Tb-8]** confirmed the removal of the galactopyranose residue of **[Tb-5]** with a concomitant luminescence decrease (data not shown). The kinetic parameters for the enzyme reaction of **[Tb-5]** with β-galactosidase were determined by measuring the luminescence change of **[Tb-5]**, because it is well known that the linear relationship of the longitudinal relaxation rates, $1/T_1$, of the water protons is valid only if the concentration of the paramagnetic species, Gd^{3+}, is at the level of mmol or submmol per kilogram of solvent (millimolality or submillimolality),[2] whereas for the determination of the ki-

netic parameters, the β-galactosidase substrate concentration should be in the range of several μM≈several hundred μM. Kinetic parameters K_m and k_{cat} were determined by direct fitting of the initial velocity versus substrate concentration data to the Michaelis–Menten equation (see Supporting Information). The values of K_m, k_{cat}, and k_{cat}/K_m of **[Tb-5]** for β-galactosidase were 81.6 μM, 2.7 s^{-1}, and 33.1 $mM^{-1}s^{-1}$, respectively. For reference, the values for *o*-nitrophenyl β-D-galactoside (ONPG) and phenyl β-D-galactoside (PG) for β-galactosidase have been reported to be K_m=100 and 90 μM, k_{cat}=600 and 35 s^{-1}, k_{cat}/K_m=6000 and 389 $mM^{-1}s^{-1}$, respectively.[25] The reactivity of **[Tb-5]** for β-galactosidase is likely to be sufficient for the detection of enzyme activity in biological systems, on the basis of the kinetic parameters of ONPG and PG, and the experimental data from refs. [10a,b] and [26]. The k_{cat}/K_m value of **[Tb-5]** is probably determined by the structure of the biphenyl group which is the albumin binding moiety,[27] so it should be possible to modulate the k_{cat}/K_m value of **[Tb-5]** for β-galactosidase by modifying the structure of the albumin binding moiety. Moreover, the reactivity of **[Tb-5]** with β-galactosidase appears to be much higher than that of the β-galactosidase-activated MRI probe which was reported by Meade and co-workers.[10b]

Luminescence and chemical properties of [Tb-5] and [Tb-8]: We further investigated in the luminescence and chemical properties of **[Tb-5]** and **[Tb-8]**, and these properties are summarized in Table 2. The luminescence quantum yields (φ) of **[Tb-5]** and **[Tb-8]** were 0.4 and 0.2%, respectively, under air-equilibrated conditions (Table 2). This result corresponds to the phenomenon of the luminescence intensity decrease of **[Tb-5]** in the presence of β-galactosidase. These luminescence quantum yields are relatively low, as compared with those reported for highly luminescent lanthanide complexes,[23f,g,k] but they are sufficiently large for luminescence detection, as described above. Measurement of the decay rate constants of the Tb^{3+} excited state for **[Tb-5]** and **[Tb-8]** were carried out in both H_2O and D_2O. The luminescence lifetimes of **[Tb-5]** and **[Tb-8]** were found to be 0.77 and 0.23 ms in H_2O (τ_{H_2O}), and 1.03 and 0.43 ms in D_2O (τ_{D_2O}), respectively (Table 2). The luminescence lifetime of **[Tb-8]** which is shorter than that of **[Tb-5]** may cause the difference of luminescence intensity between **[Tb-5]** and **[Tb-8]**. These luminescence lifetimes also indicated that the numbers of coordinated water molecules (q values) at the metal center, Tb^{3+}, were 1.35 and 9.8 for **[Tb-5]** and **[Tb-8]**, respectively (Table 2), according to Equation (7).[29a,b]

Number of water molecules :

$$q^{Tb} = 5(1/\tau_{H_2O} - 1/\tau_{D_2O} - 0.06) \quad (7)$$

The q value of **[Tb-5]** is reasonable, considering the experimental data of longitudinal relaxation time (T_1) and long-lived luminescence measurements in this paper, and indicates that **[Tb-5]** has approximately one water molecule coordinated to the chelated Tb^{3+}. Further, in general, the lanthanide trivalent ion (Ln^{3+}) (such as, Eu^{3+}, Gd^{3+}, Tb^{3+}) complexes of DTPA-monoamide or DTPA-bisamide derivatives, which have a coordination number of eight for Ln^{3+}, have approximately one metal-bound water molecule.[4,21a,23f,30] However, the q value of **[Tb-8]** was extremely large, 9.8, showing inconsistency with other experimental data herein, and therefore this calculated value seems not to reflect the number of water molecules coordinated to the central metal ion, Tb^{3+}. Other factors could account for this extremely large q value of **[Tb-8]**, and the mechanism of this abnormal feature of **[Tb-8]** is now under investigation.

Table 2. Luminescence and chemical properties.

Compound	φ [%][a]	τ_{H_2O} [ms][b]	τ_{D_2O} [ms][c]	q[d]
[Tb-5]	0.4	0.77	1.03	1.35
[Tb-8]	0.2	0.23	0.43	–[e]

[a] Quantum yields were calculated by using quinine sulfate (φ=0.546 in 1N H_2SO_4)[28] as a standard, and measured in 100 mM HEPES buffer; pH 7.4. [b] In H_2O-based buffer (100 mM HEPES buffer, pH 7.4). [c] In D_2O-based buffer (100 mM HEPES buffer, pD 7.4). [d] The q values were estimated by using the equation $q^{Tb}=5(1/\tau_{H_2O}-1/\tau_{D_2O}-0.06)$, which allows for the contribution of unbound water molecules.[29a,b] [e] The chelated q value of **[Tb-8]** was extremely large (9.8), and this value seems not to reflect the number of coordinated water molecules to the centered metal ion, Tb^{3+}. Other factors may account for this extremely large q value.

Conclusion

The Gd^{3+} complex **[Gd-5]** is the first RIME-based β-galactosidase-activated MRI contrast agent, and our design strategy should be applicable to a range of new types of β-galactosidase-activated MRI contrast agents, which may possess novel chemical characteristics, such as, various reactivity with β-galactosidase, specific biodistribution in living specimens and cells, differing extent of r_1 relaxivity change, and so on. This bioactive MRI contrast agent **[Gd-5]** should be useful for studies on the gene expression of lacZ in biological systems.[1a,8,10]

Experimental Section

All reagents were purchased from Tokyo Kasei Kogyo Co. Ltd. (Japan), Wako Pure Chemical Industries Ltd. (Japan), or Aldrich Chemical Co. Inc. (St. Louis, MO), and were used directly without further purification. All solvents were used after distillation. β-Galactosidase [EC 3.2.1.23] Sigma cat G 6008 (Grade VI: From *Escherichia coli*), HSA (human serum albumin, 97–99%) Sigma cat A 9511 (1×crystallized and lyophilized), albumin from rat serum Sigma cat A 6272, BSA (bovine serum albumin) Sigma cat A 7906 (minimum 98% electrophoresis), and albumin from rabbit serum Sigma cat A 0764 (ca. 99% agarose gel electrophoresis) were purchased from Sigma. Dulbecco's phosphate-buffered saline (D-PBS(–)) Sigma cat 14190–136 was purchased from GIBCO, and was used as phosphate-buffered saline (PBS). Silica gel column chromatography was performed by using BW-300, and Chromatorex-ODS (both from Fuji Silysia Chemical Ltd., Japan). Amberlite IR-120 Plus(H) was purchased from ICN Biomedicals, Inc. (USA). Chelex 100 resin (100–200 mesh, sodium form) was purchased from Bio-Rad Laboratories (USA).

Instruments: ^1H and ^{13}C NMR spectra were recorded by using a JEOL JNM-LA300 spectrometer. Mass spectra were measured by using a JEOL-T100LC AccuTOF mass spectrometer (ESI^+ and ESI^-). HPLC

purification was performed on a reversed-phase column, Inertsil Prep-ODS 30 mm × 250 mm (GL Sciences, Inc. (Tokyo, Japan)) fitted on a Jasco PU-1587 system. Measurements of longitudinal water proton relaxation times (T_1) were made by using an NMR analyzer operating at 20 MHz, 0.47 T (Minispec mq20, Bruker). Time-resolved luminescence spectra were recorded by using a Perkin–Elmer LS-55 (Beaconsfield, Buckinghamshire, England). UV/Vis spectra were obtained by using a Shimadzu UV-1650PC (Tokyo, Japan). Normal fluorescence spectra were measured by using a Hitachi F4500 spectrofluorometer (Tokyo, Japan). Aqueous solutions of Tb^{3+} complexes illuminated at 254 nm were photographed by using a Handy UV lamp (Handy UV Lamp, SLUV-4, AS ONE Co., Japan) (see Supporting Information).

Relaxation-time measurements: The longitudinal water proton relaxation times, T_1, of aqueous solutions of the Gd^{3+} complex **[Gd-5]** or **[Gd-8]** were measured in phosphate-buffered saline (PBS, Dulbecco's phosphate-buffered saline, pH 7.4) or PBS with albumin at 20 MHz, 0.47 T (Minispec mq20, Bruker). The values of T_1 were measured from 10 points generated by using the standard inversion-recovery procedure. The r_1 relaxivity [$mM^{-1}\,s^{-1}$] of **[Gd-5]** or **[Gd-8]** was determined from the slope of the plot of $1/T_1$ versus [**[Gd-5]**] or [**[Gd-8]**] (0.25, 0.325, 0.4, and 0.475 mM) in PBS or PBS with 4.5% w/v HSA at 25 °C or 37 °C.

HPLC analysis: The transformation of **[Gd-5]** or **[Tb-5]** to **[Gd-8]** or **[Tb-8]** was monitored by using HPLC analysis. The HPLC analysis for the transformation of **[Gd-5]** to **[Gd-8]** was performed on a reversed-phase column (Inertsil ODS-3 4.6 × 250 mm (GL Sciences); eluent, a 20-min linear gradient, from 0 to 80% solvent B (solvent A, 0.1 M triethylammonium acetate (pH 6.5); solvent B, acetonitrile/H_2O 4:1); flow rate, 1.0 mL min^{-1}; UV 300 nm). The retention times of **[Gd-5]** and **[Gd-8]** under these conditions were 9.1 and 11.5 min, respectively. The HPLC analysis to measure the transformation of **[Tb-5]** to **[Tb-8]** was performed by using a reversed-phase column (Inertsil ODS-3 4.6 × 250 mm (GL Sciences); eluent, a 70-min linear gradient, from 10 to 80% solvent B (solvent A, 0.1 M triethylammonium acetate (pH 6.5); solvent B, acetonitrile/H_2O 4:1); flow rate, 1.0 mL min^{-1}; UV 280 nm). The retention times of **[Tb-5]** and **[Tb-8]** under these conditions were 7.7 and 14.9 min, respectively.

T_1 relaxation time measurements of [Gd-5] with β-galactosidase: The longitudinal relaxation T_1 times were measured for **[Gd-5]** in the presence of β-galactosidase (113 nM) or heat-inactivated β-galactosidase (10 min at 80 °C) at 113 nM, with 4.5% w/v HSA in PBS (pH 7.4), at 20 MHz, 0.47 T, at 37 °C. The concentration of β-galactosidase was calculated based on a monomer of $M_W = 116.3$ kDa.[31] On HPLC analysis of the reaction mixture, only two peaks of **[Gd-5]** and **[Gd-8]** were detected at 300 nm.

Albumin binding study: The T_1 relaxation times of **[Gd-5]** (0.1 mM) or **[Gd-8]** (0.1 mM) were measured in PBS (pH 7.4) with various concentrations of HSA (0, 0.335, 0.67, 1.005, 1.34, 1.675, 2.01, 2.345, 2.68, 3.015, and 3.35 mM). The concentrations of HSA were determined on the basis of 4.5% w/v = ≈0.67 mM.[4,11a]

Comparison of various species of serum albumins: The longitudinal water proton relaxation times T_1 of **[Gd-5]** or **[Gd-8]** were measured at 37 °C in PBS (pH 7.4) in the presence of 4.5% w/v serum albumin from four different species (human, rat, bovine, and rabbit) in the presence or absence of β-galactosidase (1.13 μM).

UV/Vis absorption spectral measurements: The absorption spectra of **[Tb-5]** (50 μM) or **[Tb-8]** (50 μM) were measured at 25 °C in aqueous solution buffered to pH 7.4 (100 mM HEPES buffer).

Time-resolved luminescence spectral measurements: The time-resolved luminescence spectra of **[Tb-5]** or **[Tb-8]** (50 μM, respectively) were measured in 100 mM HEPES buffer at pH 7.4, 25 °C (excitation at 280 nm for **[Tb-5]** and **[Tb-8]**, respectively). The slit width was 10 nm for both excitation and emission. A delay time of 50 μs and a gate time of 1.00 ms were used.

Kinetic studies: Kinetic parameters K_m and k_{cat} were determined by direct fitting of the initial velocity versus substrate (**[Tb-5]**) concentration data to the Michaelis–Menten equation as shown in the Supporting Information. The initial velocities were determined by monitoring the decrease of the Tb^{3+} luminescence of **[Tb-5]** solutions at 37 °C in PBS (pH 7.4) (excitation 280 nm, emission 545 nm) with a Hitachi F4500 spectrofluorometer, in the presence of β-galactosidase (151 nM) and various concentrations of **[Tb-5]** (5, 10, 20, 40, 80, and 160 μM). The slit width was 5 nm for both excitation and emission. The photomultiplier voltage was 700 V.

Quantum yield measurements: The luminescence spectra were measured with a Hitachi F4500 spectrofluorometer. The slit width was 2.5 nm for both excitation and emission. The photomultiplier voltage was 700 V. The luminescence spectra of **[Tb-5]** or **[Tb-8]** were measured in 100 mM HEPES buffer at pH 7.4, 25 °C, with irradiation at 280 nm. The quantum yields of Tb^{3+} complexes were evaluated by using a relative method with reference to a luminescence standard, quinine sulfate ($\varphi = 0.546$ in 1 N H_2SO_4).[28] The quantum yields of Tb^{3+} complexes can be expressed by Equation (9)[32]:

$$\Phi_x/\Phi_{st} = [A_{st}/A_x][n_x^2/n_{st}^2][D_x/D_{st}] \quad (8)$$

where Φ is the quantum yield (subscript "st" stands for the reference and "x" for the sample), A is the absorbance at the excitation wavelength, n is the refractive index, and D is the peak area (on an energy scale) of the luminescence spectra. The samples and the reference were excited at the same wavelength (280 nm). The sample and the reference absorbance at the excitation wavelength were kept as low as possible to avoid fluorescence errors ($A_{exc} < 0.05$).

Luminescence lifetime measurements: The luminescence lifetimes of the Tb^{3+} complexes were recorded on a Perkin–Elmer LS-55 instrument. The data were collected with a 10-μsec resolution in H_2O (100 mM HEPES buffer at pH 7.4) and D_2O (100 mM HEPES buffer at pD 7.4, based on the equation pD = pH + 0.40[33]) at 25 °C, and fitted to a single-exponential curve obeying Equation (9):

$$I = I_0 \exp(-t/\tau) \quad (9)$$

where I_0 and I are the luminescence intensities at the time $t = 0$ and time t, respectively, and τ is the luminescence emission lifetime. Lifetimes were obtained by monitoring the emission intensity at 545 nm (excitation at 280 nm).

Acknowledgement

This work was supported by the Ministry of Education, Culture, Sports, Science and Technology of Japan (Grants for The Advanced and Innovational Research Program in Life Sciences, 16370071 and 16659003 to T.N., 15681012, 17035019, 17036012, 017048006, and 17651119 to K.K.). T.N. was also supported by the Hoh-ansha Foundation. K.K. was also supported by the Sankyo Foundation, by the Kanagawa Academy of Science, and by the Shimadzu Foundation. K.H. was the recipient of Research Fellowships of the Japan Society for the Promotion of Science for Young Scientists. We thank Professor Haruhiko Bito for valuable suggestions.

[1] a) G. Genove, U. DeMarco, H. Xu, W. F. Goins, E. T. Ahrens, *Nat. Med.* **2005**, *11*, 450–454; b) K. H. Thompson, C. Orvig, *Science* **2003**, *300*, 936–939; c) K. Nakahara, T. Hayashi, S. Konishi, Y. Miyashita, *Science* **2002**, *295*, 1532–1536; d) H. Degani, V. Gusis, D. Weinstein, S. Fields, S. Strano, *Nat. Med.* **1997**, *3*, 780–782; e) R. E. Jacobs, S. E. Fraser, *Science* **1994**, *263*, 681–684; f) J. C. Frias, K. J. Williams, E. A. Fisher, Z. A. Fayad, *J. Am. Chem. Soc.* **2004**, *126*, 16316–16317.

[2] A. E. Merbach, É. Tóth, *The Chemistry of Contrast Agents in Medical Magnetic Resonance Imaging*, Wiley, New York, **2001**.

[3] a) S. Aime, M. Botta, M. Fasano, E. Terreno, *Acc. Chem. Res.* **1999**, *32*, 941–949; b) S. Aime, M. Botta, M. Fasano, E. Terreno, *Chem. Soc. Rev.* **1998**, *27*, 19–29.

[4] P. Caravan, J. J. Ellison, T. J. McMurry, R. B. Lauffer, *Chem. Rev.* **1999**, *99*, 2293–2352.

[5] V. M. Runge, D. Y. Gelblum, M. L. Pacetti, F. Carolan, G. Heard, *Radiology* **1990**, *177*, 393–400.

[6] a) M. P. Lowe, *Aust. J. Chem.* **2002**, *55*, 551–556; b) L. Thunus, R. Lejeune, *Coord. Chem. Rev.* **1999**, *184*, 125–155; c) V. Comblin, D. Gilsoul, M. Hermann, V. Humblet, V. Jacques, M. Mesbahi, C. Sauvage, J. F. Desreux, *Coord. Chem. Rev.* **1999**, *185–186*, 451–470; d) M. K. Thompson, B. Misselwitz, L. S. Tso, D. M. J. Doble, H. Schmitt-Willich, K. N. Raymond, *J. Med. Chem.* **2005**, *48*, 3874–3877; e) V. C. Pierre, M. Botta, K. N. Raymond, *J. Am. Chem. Soc.* **2005**, *127*, 504–505; f) H. Kato, Y. Kanazawa, M. Okumura, A. Taninaka, T. Yokawa, H. Shinohara, *J. Am. Chem. Soc.* **2003**, *125*, 4391–4397; g) M. Mikawa, H. Kato, M. Okumura, M. Narazaki, Y. Kanazawa, N. Miwa, H. Shinohara, *Bioconjugate Chem.* **2001**, *12*, 510–514; h) A. Accardo, D. Tesauro, P. Roscigno, E. Gianolio, L. Paduano, G. D'Errico, C. Pedone, G. Morelli, *J. Am. Chem. Soc.* **2004**, *126*, 3097–3107; i) J. Lee, M. J. Zylka, D. J. Anderson, J. E. Burdette, T. K. Woodruff, T. J. Meade, *J. Am. Chem. Soc.* **2005**, *127*, 13164–13166.

[7] a) T. J. Meade, A. K. Taylor, S. R. Bull, *Curr. Opin. Neurobiol.* **2003**, *13*, 597–602; b) J. A. Duimstra, F. J. Femia, T. J. Meade, *J. Am. Chem. Soc.* **2005**, *127*, 12847–12855; c) W. Li, S. E. Fraser, T. J. Meade, *J. Am. Chem. Soc.* **1999**, *121*, 1413–1414; d) W. Li, G. Parigi, M. Fragai, C. Luchinat, T. J. Meade, *Inorg. Chem.* **2002**, *41*, 4018–4024; e) S. Zhang, K. Wu, A. D. Sherry, *Angew. Chem.* **1999**, *111*, 3382–3384; *Angew. Chem. Int. Ed.* **1999**, *38*, 3192–3194; f) N. Raghunand, C. Howison, A. D. Sherry, S. Zhang, R. J. Gillies, *Magn. Reson. Med.* **2003**, *49*, 249–257; g) É. Tóth, R. D. Bolskar, A. Borel, G. González, L. Helm, A. E. Merbach, B. Sitharaman, L. J. Wilson, *J. Am. Chem. Soc.* **2005**, *127*, 799–805; h) M. Mikawa, N. Miwa, M. Bräutigam, T. Akaike, A. Maruyama, *J. Biomed. Mater. Res.* **2000**, *49*, 390–395; i) M. Mikawa, T. Yokawa, N. Miwa, M. Brautigam, T. Akaike, A. Maruyama, *Acad. Radiol.* **2002**, *9*, S109–S111; j) K. E. Løkling, R. Skurtveit, A. Bjørnerud, S. L. Fossheim, *Magn. Reson. Med.* **2004**, *51*, 688–696; k) S. Aime, M. Botta, E. Gianolio, E. Terreno, *Angew. Chem.* **2000**, *112*, 763–766; *Angew. Chem. Int. Ed.* **2000**, *39*, 747–750; l) K. Hanaoka, K. Kikuchi, Y. Urano, M. Narazaki, T. Yokawa, S. Sakamoto, K. Yamaguchi, T. Nagano, *Chem. Biol.* **2002**, *9*, 1027–1032; m) K. Hanaoka, K. Kikuchi, Y. Urano, T. Nagano, *J. Chem. Soc. Perkin Trans. 2* **2001**, 1840–1843; n) R. Trokowski, S. Zhang, A. D. Sherry, *Bioconjugate Chem.* **2004**, *15*, 1431–1440.

[8] a) D. Högemann, J. P. Basilion, *Eur. J. Nucl. Med.* **2002**, *29*, 400–408; b) R. Weissleder, A. Moore, R. Mahmood, R. Bhorade, H. Benveniste, E. A. Chiocca, J. P. Basilion, *Nat. Med.* **2000**, *6*, 351–354.

[9] D. J. Spergel, U. Krüth, D. R. Shimshek, R. Sprengel, P. H. Seeburg, *Prog. Neurobiol.* **2001**, *63*, 673–686.

[10] a) A. Y. Louie, M. M. Hüber, E. T. Ahrens, U. Rothbächer, R. Moats, R. E. Jacobs, S. E. Fraser, T. J. Meade, *Nat. Biotechnol.* **2000**, *18*, 321–325; b) R. A. Moats, S. E. Fraser, T. J. Meade, *Angew. Chem.* **1997**, *109*, 749–752; *Angew. Chem. Int. Ed. Engl.* **1997**, *36*, 726–728; c) M. M. Alauddin, A. Y. Louie, A. Shahinian, T. J. Meade, P. S. Conti, *Nucl. Med. Biol.* **2003**, *30*, 261–265.

[11] a) P. Cravan, N. J. Cloutier, M. T. Greenfield, S. A. McDermid, S. U. Dunham, J. W. M. Bulte, J. C. Amedio, Jr., R. J. Looby, R. M. Supkowski, W. Dew. Horrocks, Jr., T. J. McMurry, R. B. Lauffer, *J. Am. Chem. Soc.* **2002**, *124*, 3152–3162; b) S. Amie, E. Gianolio, E. Terreno, G. B. Giovenzana, R. Pagliarin, M. Sisti, G. Palmisano, M. Botta, M. P. Lowe, D. Parker, *J. Biol. Inorg. Chem.* **2000**, *5*, 488–497; c) S. Aime, M. Botta, S. G. Crich, G. B. Giovenzana, R. Pagliarin, M. Piccinini, M. Sisti, E. Terreno, *J. Biol. Inorg. Chem.* **1997**, *2*, 470–479.

[12] R. B. Lauffer, T. J. McMurry, S. O. Dunham, D. M. Scott, D. J. Parmelee, S. Dumas, PCT Int. Appl. WO 9736619, **1997**.

[13] A. L. Nivorozhkin, A. F. Kolodziej, P. Caravan, M. T. Greenfield, R. B. Lauffer, T. J. McMurry, *Angew. Chem.* **2001**, *113*, 2987–2990; *Angew. Chem. Int. Ed.* **2001**, *40*, 2903–2906.

[14] L. M. De León-Rodríguez, A. Ortiz, A. L. Weiner, S. Zhang, Z. Kovacs, T. Kodadek, A. D. Sherry, *J. Am. Chem. Soc.* **2002**, *124*, 3514–3515.

[15] P. L. Anelli, I. Bertini, M. Fragai, L. Lattuada, C. Luchinat, G. Parigi, *Eur. J. Inorg. Chem.* **2000**, 625–630.

[16] L. Josephson, J. M. Perez, R. Weissleder, *Angew. Chem.* **2001**, *113*, 3304–3306; *Angew. Chem. Int. Ed.* **2001**, *40*, 3204–3206.

[17] J. W. Chen, W. Pham, R. Weissleder, A. Bogdanov, Jr., *Magn. Reson. Med.* **2004**, *52*, 1021–1028.

[18] M. Zhao, L. Josephson, Y. Tang, R. Weissleder, *Angew. Chem.* **2003**, *115*, 1413–1416; *Angew. Chem. Int. Ed.* **2003**, *42*, 1375–1378.

[19] S. Aime, M. Chiaussa, G. Digilio, E. Gianolio, E. Terreno, *J. Biol. Inorg. Chem.* **1999**, *4*, 766–774.

[20] S. Aime, M. Botta, M. Fasano, S. G. Crich, E. Terreno, *J. Biol. Inorg. Chem.* **1996**, *1*, 312–319.

[21] a) D. Parker, J. A. G. Williams, *J. Chem. Soc. Dalton Trans.* **1996**, 3613–3628; b) D. Parker, *Coord. Chem. Rev.* **2000**, *205*, 109–130; c) G. R. Choppin, D. R. Peterman, *Coord. Chem. Rev.* **1998**, *174*, 283–299.

[22] P. R. Selvin, T. M. Rana, J. E. Hearst, *J. Am. Chem. Soc.* **1994**, *116*, 6029–6030.

[23] a) I. Hemmilä, S. Webb, *Drug Discovery Today* **1997**, *2*, 373–381; b) A. J. Kolb, P. V. Kaplita, D. J. Hayes, Y. W. Park, C. Pernell, J. S. Major, G. Mathis, *Drug Discovery Today* **1998**, *3*, 333–342; c) V. Laitala, I. Hemmilä, *Anal. Chem.* **2005**, *77*, 1483–1487; d) J. Karvinen, V. Laitala, M. L. Mäkinen, O. Mulari, J. Tamminen, J. Hermonen, P. Hurskainen, I. Hemmilä, *Anal. Chem.* **2004**, *76*, 1429–1436; e) Y. Koshi, E. Nakata, I. Hamachi, *ChemBioChem* **2005**, *6*, 1349–1352; f) K. Hanaoka, K. Kikuchi, H. Kojima, Y. Urano, T. Nagano, *J. Am. Chem. Soc.* **2004**, *126*, 12470–12476; g) N. Weibel, L. J. Charbonnière, M. Guardigli, A. Roda, R. Ziessel, *J. Am. Chem. Soc.* **2004**, *126*, 4888–4896; h) M. K. Johansson, R. M. Cook, J. Xu, K. N. Raymond, *J. Am. Chem. Soc.* **2004**, *126*, 16451–16455; i) Z. Lin, M. Wu, M. Schäferling, O. S. Wolfbeis, *Angew. Chem.* **2004**, *116*, 1767–1770; *Angew. Chem. Int. Ed.* **2004**, *43*, 1735–1738; j) K. Lee, V. Dzubeck, L. Latshaw, J. P. Schneider, *J. Am. Chem. Soc.* **2004**, *126*, 13616–13617; k) S. Mameri, L. J. Charbonnière, R. F. Ziessel, *Inorg. Chem.* **2004**, *43*, 1819–1821; l) C. Li, G. L. Law, W. T. Wong, *Org. Lett.* **2004**, *6*, 4841–4844; m) J. C. Frias, G. Bobba, M. J. Cann, C. J. Hutchison, D. Parker, *Org. Biomol. Chem.* **2003**, *1*, 905–907; n) K. J. Franz, M. Nitz, B. Imperiali, *ChemBioChem* **2003**, *4*, 265–271; o) J. P. Cross, M. Lauz, P. D. Badger, S. Petoud, *J. Am. Chem. Soc.* **2004**, *126*, 16278–16279.

[24] D. Parker, R. S. Dickins, H. Puschmann, C. Crossland, J. A. K. Howard, *Chem. Rev.* **2002**, *102*, 1977–2010.

[25] O. Viratelle, J. P. Tenu, J. Garnier, J. Yon, *Biochem. Biophys. Res. Commun.* **1969**, *37*, 1036–1041.

[26] a) Y. Urano, M. Kamiya, K. Kanda, T. Ueno, K. Hirose, T. Nagano, *J. Am. Chem. Soc.* **2005**, *127*, 4888–4894; b) J. Hofmann, M. Sernetz, *Anal. Biochem.* **1983**, *131*, 180–186.

[27] J. P. Tenu, O. M. Viratelle, J. Garnier, J. Yon, *Eur. J. Biochem.* **1971**, *20*, 363–370.

[28] W. H. Helhuish, *J. Phys. Chem.* **1961**, *65*, 229–235.

[29] a) A. Beeby, I. M. Clarkson, R. S. Dickins, S. Faulkner, D. Parker, L. Royle, A. S. de Sousa, J. A. G. Williams, M. Woods, *J. Chem. Soc. Perkin Trans. 2* **1999**, 493–503; b) S. Quici, G. Marzanni, M. Cavazzini, P. L. Anelli, M. Botta, E. Gianolio, G. Accorsi, N. Armaroli, F. Barigelletti, *Inorg. Chem.* **2002**, *41*, 2777–2784.

[30] M. Li, P. R. Selvin, *J. Am. Chem. Soc.* **1995**, *117*, 8132–8138.

[31] A. V. Fowler, I. Zabin, *J. Biol. Chem.* **1978**, *253*, 5521–5525.

[32] Q. Y. Chen, C. J. Feng, Q. H. Luo, C. Y. Duan, X. S. Yu, D. J. Liu, *Eur. J. Inorg. Chem.* **2001**, 1063–1069.

[33] Y. M. Wang, Y. J. Wang, Y. L. Wu, *Polyhedron* **1999**, *18*, 109–117.

Received: May 24, 2007
Published online: November 8, 2007

JACS
JOURNAL OF THE AMERICAN CHEMICAL SOCIETY

Communication

Lanthanide-Based Protease Activity Sensors for Time-Resolved Fluorescence Measurements

Shin Mizukami, Kazuhiro Tonai, Masahiro Kaneko, and Kazuya Kikuchi

J. Am. Chem. Soc., **2008**, 130 (44), 14376-14377• DOI: 10.1021/ja800322b • Publication Date (Web): 08 October 2008

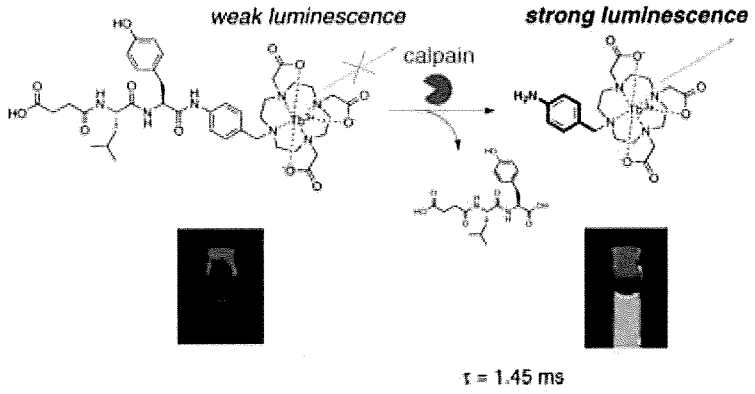

More About This Article

Additional resources and features associated with this article are available within the HTML version:

- Supporting Information
- Access to high resolution figures
- Links to articles and content related to this article
- Copyright permission to reproduce figures and/or text from this article

View the Full Text HTML

J|A|C|S
COMMUNICATIONS

Published on Web 10/08/2008

Lanthanide-Based Protease Activity Sensors for Time-Resolved Fluorescence Measurements

Shin Mizukami, Kazuhiro Tonai, Masahiro Kaneko, and Kazuya Kikuchi*

Division of Advanced Science and Biotechnology, Graduate School of Engineering, Osaka University, 2-1 Yamadaoka, Suita, Osaka 565-0871, Japan

Received January 15, 2008; E-mail: kkikuchi@mls.eng.osaka-u.ac.jp

Time-resolved fluorescence measurements with long-lifetime luminescent lanthanide complexes[1] have attracted great attention from scientists. This is because the time-resolved luminescence signals are highly sensitive and are scarcely affected by other fluorescent compounds that coexist in the sample, which often interfere with steady-state fluorescence measurements. This method is quite useful, especially in high-throughput drug screening.[2] Protease inhibitors can be important drug targets for diverse diseases, including cancer, AIDS, inflammatory disorders, and so on. Therefore, lanthanide-based luminescent sensors that detect protease activities assume great significance.

Karvinen et al. reported a protease assay based on time-resolved fluorescence resonance energy transfer (TR-FRET).[3] However, the synthesis of TR-FRET probes is generally laborious because it involves the attachment of both the luminescent lanthanide complex and the appropriate quencher on the substrate peptides. Additionally, when the probe concentration is high, this system is associated with the risk of diffusion-enhanced intermolecular FRET.[4] Although another simpler assay based on quenching by photoinduced electron transfer is known, the luminescent substrate becomes nonluminescent after enzyme reaction in this case.[5] In principle, such quenching-type fluorescent probes are inferior to fluorogenic probes, which fluoresce after enzyme reaction, because fluorescence is generally quenched by several factors such as collisional quenching, energy transfer, electron transfer, and so on. Besides TR-FRET probes, there exist no other fluorogenic protease probes based on lanthanide luminescence. Therefore, fluorogenic probes such as substrate peptides attached with the short-lifetime fluorophore MCA (4-methylcoumarinyl-7-amide) are widely used in protease assays, despite the above-described limitations.[6] We here report simple-structure luminogenic lanthanide probes that detect protease activities.

The long-lifetime luminescence of lanthanide ions is due to the forbidden f−f transitions of metal electrons. Generally, energy transfer from an adjacent chromophore to a lanthanide ion is utilized for the efficient excitation of lanthanide ions. The structures of the antenna chromophores regulate the lanthanide luminescence intensity.[7] Thus, the antenna groups can be strategic targets for designing luminogenic lanthanide probes. By modifying the antenna structures, several kinds of lanthanide-based probes have been developed so far, for instance, for detecting pH,[8] metal ions,[9] and other molecules.[10] To develop luminogenic lanthanide probes for detecting protease activities, the candidate antenna groups should fulfill two requirements: (1) antenna groups with an amino group should yield strong lanthanide luminescence and (2) the lanthanide luminescence should be very weak when the amino group is protected with an acyl group. We thoroughly investigated the known antenna groups for the above requirements. We found that very few antenna groups that have an amino group could emit lanthanide luminescence in aqueous solution.[11] We considered this is because

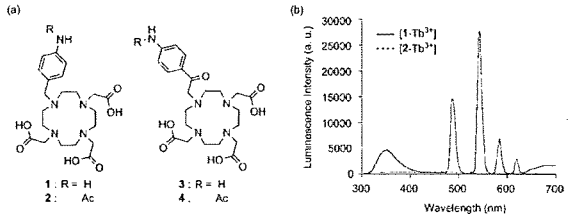

Figure 1. (a) Structures of synthesized compounds; (b) emission spectra of [**1**-Tb^{3+}] and [**2**-Tb^{3+}]; λ_{ex} = 250 nm.

Scheme 1. Structures and Schematic Representation of the Probes for Detecting Protease Activity

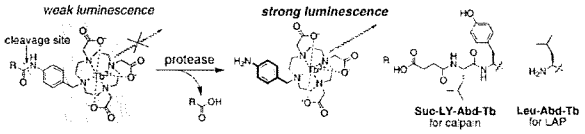

amino groups generally function as quenching groups for lanthanide luminescence.[5,12,13] Generally, amino substituents cause the red shift of the absorption spectra, and long-wavelength dyes are not adequate for the efficient excitation of Tb^{3+} or Eu^{3+}.[12] Thus, we hypothesized that only simple aromatic compounds with an amino group can act as efficient antenna groups for luminescent lanthanide ions such as Tb^{3+} and Eu^{3+}. Since tyrosine is known to sensitize Tb^{3+} and Eu^{3+},[14] we expected that even aniline derivatives could serve as good antenna groups.

For confirming the hypothesis, we designed and synthesized antenna-chelator conjugates **1** and **3**, which have simple aniline derivative groups as the antennas, and the corresponding acetylated compounds **2** and **4** (Figure 1a). We chose DO3A (1,4,7-tricarboxymethyl-1,4,7,10-tetraazacyclododecane) as the chelator for its strong binding ability to trivalent lanthanide ions.[15] The complex [**1**-Tb^{3+}] showed the characteristic emission spectrum of lanthanide complexes besides the antenna fluorescence at 350 nm (Figure 1b). Meanwhile, [**2**-Tb^{3+}]—the Tb^{3+} complex of the acetylated compound **2**—did not show lanthanide luminescence. On the other hand, although [**3**-Tb^{3+}] did not show lanthanide luminescence, [**4**-Tb^{3+}] showed strong lanthanide luminescence (see Supporting Information). Since the two acetylated compounds **2** and **4** are the model compounds of peptide conjugates, the above results indicated that the 4-aminobenzyl group can be a suitable antenna for luminogenic lanthanide probes detecting protease activities and that 4-aminobenzoylmethyl group can be an antenna for quenching-type protease probes. In addition, none of the Eu^{3+} complexes of compounds **1**−**4** showed lanthanide luminescence (data not shown).

Next, we designed Suc-LY-Abd-Tb to detect calpain activity, as shown in Scheme 1. Calpains are a family of intracellular cysteine proteases that are involved in many cellular processes.[16] Calpains

10.1021/ja800322b CCC: $40.75

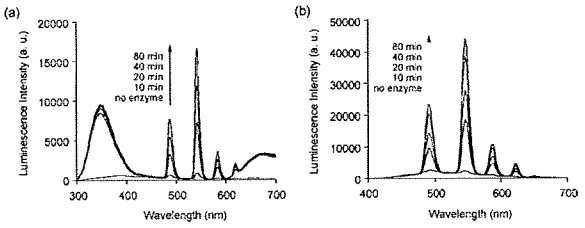

Figure 2. (a) Steady-state and (b) time-resolved (delay time, 10 μs; gate time, 3.0 ms) emission spectral change of Suc-LY-Abd-Tb with calpain I. λ_{ex} = 250 nm.

Table 1. Photophysical Properties of the Synthesized Compounds

	λ_{abs}/nm	ϵ/M^{-1} cm^{-1}	Φ	τ/ms
[**1**-Tb^{3+}]	240	12 000	0.051	1.47
[**2**-Tb^{3+}]	284	3 500	<0.001	1.49
Suc-LY-Abd-Tb	254	11 000	<0.001	1.46
Suc-LY-Abd-Tb + calpain I[a]	263	13 000	0.012	1.45

[a] It was confirmed by reversed-phase HPLC that enzyme reaction was completed.

are also related to several diseases such as muscular dystrophy, Alzheimer's disease, Parkinson's disease, and so on.[17] Thus, highly sensitive detection methods for calpain activities are crucial for developing drugs for such diseases.[18] The peptide sequence Suc-LY is known to be recognized efficiently by both calpains I and II.[17] The peptide-ligand conjugate Suc-LY-Abd was synthesized by a liquid-phase method, and the ligand was then complexed with Tb^{3+}. As we expected, the emission spectrum of Suc-LY-Abd-Tb was scarcely luminescent, similar to that of [**2**-Tb^{3+}]. Then, the addition of calpain I to the Suc-LY-Abd-Tb solution increased the emission intensity in a time-dependent manner (Figure 2a). The steady-state spectra in Figure 2a also include fluorescence around 350 nm derived from the antenna and the protein. In such cases, time-resolved measurement is very effective. The luminescence lifetimes of the synthesized compounds were approximately 1.5 ms (Table 1), much longer than those of general organic fluorescent compounds. Thus, the short-lifetime components in the emission spectra were completely excluded by performing measurements after a delay of 10 μs (Figure 2b).

We investigated the practical usefulness of Suc-LY-Abd-Tb. When fluorescent molecules are present in samples, they are very likely to significantly affect the results of fluorescence assays. For example, fluorescent drug candidates would give rise to false results for enzyme screening assays. We performed calpain assays with Suc-LY-Abd-Tb and the commercial probe Suc-LY-MCA in the presence of fluorescent compounds such as umbelliferone. The fluorescence intensity of Suc-LY-MCA was considerably increased in the presence of such compounds as compared to that in their absence. The time-resolved fluorescence intensity of Suc-LY-Abd-Tb was barely affected under the same conditions (see Supporting Information). This result indicates the superiority of our lanthanide-based probes over conventional fluorescent probes in practical applications.

Finally, to demonstrate the generality of our sensing system, we synthesized another lanthanide-based probe, Leu-Abd-Tb, for leucine aminopeptidase (LAP); this enzyme hydrolyzes the peptide bond of N-terminal hydrophobic amino acids such as leucine (Scheme 1). Leu-Abd-Tb showed an increase in the time-resolved luminescence when incubated with LAP (see Supporting Information), similar to the case of Suc-LY-Abd.

In conclusion, we developed novel luminogenic lanthanide probes for detecting protease activities. The probe design principle could be widely applicable to time-resolved assays for any proteases. These lanthanide-based probes could accelerate drug-screening processes and also contribute to the clarification of biological systems. Furthermore, achievement of longer wavelength excitation could enable a microscopic time-resolved fluorescence imaging of protease activities in living cells.[13]

Acknowledgment. We thank MEXT of Japan and JST for the financial supports. We thank Dr. Tomoyoshi Suenobu for the technical support for time-resolved fluorescence measurement.

Supporting Information Available: Detailed synthetic procedures; supplementary spectra; physical properties; photostability experiment; enzyme reaction experiment. This material is available free of charge via the Internet at http://pubs.acs.org.

References

(1) (a) Bünzli, J.-C. G.; Piguet, C. *Chem. Soc. Rev.* **2005**, *34*, 1048–1077. (b) Yuan, J.; Wang, G. *Trends Anal. Chem.* **2006**, *25*, 490–500.
(2) Kumar, R. A.; Clark, D. S. *Curr. Opin. Chem. Biol.* **2006**, *10*, 162–168.
(3) (a) Karvinen, J.; Laitala, V.; Mäkinen, M.-L.; Mulari, O.; Tamminen, J.; Hermonen, J.; Hurskainen, P.; Hammilä, I. *Anal. Chem.* **2004**, *76*, 1429–1436. (b) Karvinen, J.; Elomaa, A.; Mäkinen, M. -L.; Hakala, H.; Mukkala, V. -M.; Peuralahti, J.; Hurskainen, P.; Hovinen, J.; Hemmilä, I. *Anal. Biochem.* **2004**, *325*, 317–325.
(4) Stryer, L.; Thomas, D. D.; Meares, C. F. *Annu. Rev. Biophys. Bioeng.* **1982**, *11*, 203–222.
(5) Terai, T.; Kikuchi, K.; Iwasawa, S.; Kawabe, T.; Hirata, Y.; Urano, Y.; Nagano, T. *J. Am. Chem. Soc.* **2006**, *128*, 6938–6946.
(6) (a) Rano, T. A.; Timkey, T.; Peterson, E. P.; Rotonda, J.; Nicholson, D. W.; Becker, J. W.; Chapman, K. T.; Thornberry, N. A. *Chem. Biol.* **1997**, *4*, 149–155. (b) Harris, J. L.; Backes, B. J.; Leonetti, F.; Mahrus, S.; Ellman, J. A.; Craik, C. S. *Proc. Natl. Acad. Sci. U.S.A.* **2000**, *97*, 7754–7759. (c) Salisbury, C. M.; Maly, D. J.; Ellman, J. A. *J. Am. Chem. Soc.* **2002**, *124*, 14868–14870.
(7) Latva, M.; Takalo, H.; Mukkala, V. -M.; Matachescu, C.; Rodriguez-Ubis, J. C.; Kankare, J. *J. Lumin.* **1997**, *75*, 149–169.
(8) (a) de Silva, A. P; Gunaratne, H. Q. N.; Rice, T. E. *Angew. Chem., Int. Ed. Engl.* **1996**, *35*, 2116–2118. (b) Parker, D.; Senanayake, P. K.; Williams, J. A. G. *J. Chem. Soc., Perkin Trans. 2* **1998**, 2129–2139. (c) Gunnlaugsson, T.; Mac Dónaill, D. A.; Parker, D. *J. Am. Chem. Soc.* **2001**, *123*, 12866–12876. (d) Gunnlaugsson, T.; Leonard, J. P.; Sénéchal, K.; Harte, A. J. *J. Am. Chem. Soc.* **2004**, *126*, 12470–12476.
(9) (a) de Silva, A. P; Gunaratne, H. Q. N.; Rice, T. E.; Stewart, S. *Chem. Commun.* **1997**, 1891–1892. (b) Reany, O.; Gunnlaugsson, T.; Parker, D. *J. Chem. Soc., Perkin Trans 2* **2000**, 1819–1831. (c) Hanaoka, K.; Kikuchi, K.; Kojima, H.; Urano, Y.; Nagano, T. *J. Am. Chem. Soc.* **2004**, *126*, 12470–12476.
(10) (a) Bobba, G.; Frias, J. C.; Parker, D. *Chem. Commun.* **2002**, 890–891. (b) Hamblin, J.; Abboyi, N.; Lowe, M. P. *Chem. Commun.* **2005**, 657–659.
(11) Lamture, J. B.; Zhou, Z. H.; Kumar, A. S.; Wensel, T. G. *Inorg. Chem.* **1995**, *34*, 864–869.
(12) Latva, M.; Takalo, H.; Mukkala, V. -M.; Matachescu, C.; Rodríguez-Ubis, J. C.; Kankare, J. *J. Lumin.* **1997**, *75*, 149–169.
(13) Hanaoka, K.; Kikuchi, K.; Kobayashi, S.; Nagano, T. *J. Am. Chem. Soc.* **2007**, *129*, 13502–13509.
(14) (a) Brittain, H. G.; Frederick, S. R.; Martin, R. B. *J. Am. Chem. Soc.* **1976**, *98*, 8255–8260. (b) Bruno, J.; Horrocks, W. D.; Zauher, R. J. *Biochemistry* **1992**, *31*, 7016–7026.
(15) Kumar, K.; Chang, C. A.; Tweedle, M. F. *Inorg. Chem.* **1993**, *32*, 587–593.
(16) Goll, D. E.; Thompson, V. F.; Li, H.; Wei, W.; Cong, J. *Physiol. Rev.* **2003**, *83*, 731–801.
(17) (a) Kinbara, K.; Ishiura, S.; Tomioka, S.; Sorimachi, H.; Jeong, S. Y.; Amano, S.; Kawasaki, H.; Kolmerer, B.; Kimura, S.; Labeit, S.; Suzuki, K. *Biochem. J.* **1998**, *335*, 589596. (b) Lee, M. S.; Kwon, Y. T.; Li, M.; Peng, J.; Friedlander, R. M.; Tsai, L. H. *Nature* **2000**, *405*, 360–364. (c) Mouatt-Prigent, A.; Karlsson, J. O.; Agid, Y.; Hirsch, E. C. *Neuroscience* **1996**, *73*, 979–987.
(18) (a) Sasaki, T.; Kikuchi, T.; Yumoto, N.; Yoshimura, N.; Murachi, T. *J. Biol. Chem.* **1984**, *259*, 12489–12494. (b) Jiang, S. T.; Wang, J. H.; Chang, T.; Chen, C. S. *Anal. Biochem.* **1997**, *244*, 233–238. (c) Mallya, S. K.; Meyer, S.; Bozyczko-Coyne, D.; Siman, R.; Ator, M. A. *Biochem. Biophys. Res. Commun.* **1998**, *248*, 293–296. (d) Mittoo, S.; Sundstrom, L. E.; Bradley, M. *Anal. Biochem.* **2003**, *319*, 234–238. (e) Vanderklish, P. W.; Krushel, L. A.; Holst, B. H.; Gally, J. A.; Crossin, K. L. *Proc. Natl. Acad. Sci. U.S.A.* **2000**, *97*, 2253–2258.

JA800322B

JACS
JOURNAL OF THE AMERICAN CHEMICAL SOCIETY

Communication

Covalent Protein Labeling Based on Noncatalytic #-Lactamase and a Designed FRET Substrate

Shin Mizukami, Shuji Watanabe, Yuichiro Hori, and Kazuya Kikuchi

J. Am. Chem. Soc., **Article ASAP** • DOI: 10.1021/ja8082285 • Publication Date (Web): 18 March 2009

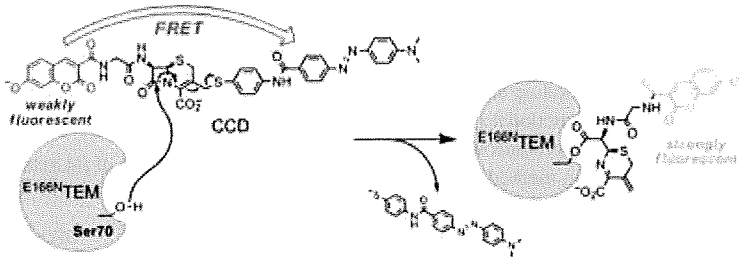

More About This Article

Additional resources and features associated with this article are available within the HTML version:

- Supporting Information
- Access to high resolution figures
- Links to articles and content related to this article
- Copyright permission to reproduce figures and/or text from this article

View the Full Text HTML

J|A|C|S
COMMUNICATIONS

Covalent Protein Labeling Based on Noncatalytic β-Lactamase and a Designed FRET Substrate

Shin Mizukami, Shuji Watanabe, Yuichiro Hori, and Kazuya Kikuchi*

Graduate School of Engineering, Osaka University, 2-1 Yamadaoka, Suita, Osaka 565-0871, Japan

Received October 20, 2008; E-mail: kkikuchi@mls.eng.osaka-u.ac.jp

Fluorescence microscopy is one of the most common techniques employed in the field of life science. With the rapid progress that has been achieved with regard to optical systems, fluorescent proteins (FPs) have acquired important roles for fluorescence microscopy experiments. In order to visualize the localization and behavior of particular proteins of interest, FPs such as green fluorescent protein (GFP) have conventionally been used.[1] More recently, techniques for labeling proteins with small molecules have attracted the attention of many life scientists because they can extend the range of natural FPs, for example, by incorporating near-infrared fluorescent dyes, MRI contrast agents, or biofunctional molecules such as biotin. Several approaches for modifying proteins with small molecules have been commercialized, including methods based on the tetracysteine tag,[2] HaloTag,[3] and SNAP-tag.[4] Other protein labeling methods involving the use of biotin ligase,[5] transglutaminase,[6] hexahistidine,[7] tetra-aspartic acid,[8] etc. have also been reported. Among the abovementioned labeling methods, only the tetracysteine tag exhibits fluorogenic properties. In the other labeling methods, it is necessary to wash the treated cells prior to microscopic measurements to eliminate background fluorescence. Thus, new labeling techniques that satisfy the dual criteria of specificity and fluorogenicity are desirable.

In this paper, we report a specific protein labeling system with an off-on fluorescence switch. It involves covalent modification of a genetically engineered hydrolytic enzyme with a rationally designed fluorogenic probe that exploits the principle of fluorescence resonance energy transfer (FRET). Using this system, we can achieve specific and fluorogenic protein labeling under physiological conditions.

First, we designed the tag protein. Plant or bacterial proteins are preferably used to achieve bioorthogonal labeling in mammalian cells. We focused on β-lactamase as the candidate tag because β-lactamases are small bacterial enzymes that hydrolyze antibiotics containing a β-lactam structure and have no endogenous counterpart among eukaryotic cells.[9] β-Lactamase has been widely used as a reporter enzyme for examining gene expression in living mammalian cells.[10] Class A β-lactamases such as the 29 kDa TEM-1[11] have been extensively investigated with regard to their structures, enzyme reaction kinetics, substrate specificity, inhibitors, etc.[12] The reaction of TEM-1 with β-lactams involves acylation and deacylation steps (Scheme 1). In the acylation step, Ser70 attacks the amide bond of the β-lactam ring to form an intermediate acyl-enzyme complex (ES*). In the deacylation step, an activated water molecule hydrolyzes the ester bond of the intermediate to yield the product. Previous studies have shown that Glu166 is essential for the deacylation step[13] and that the E166N mutant of TEM-1 (^{E166N}TEM) accumulates the acyl-enzyme intermediate by markedly slowing deacylation (k_3) relative to acylation (k_2).[14] We hoped to exploit the properties of the ^{E166N}TEM mutant to covalently attach a fluorescent substrate to β-lactamase.

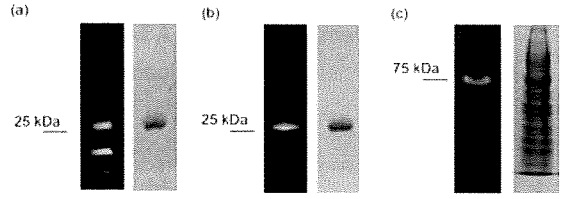

Figure 1. (a, b) Fluorescence (left) and CBB-stained (right) gel images of ^{E166N}TEM after incubation with (a) CA and (b) CCD. (c) Fluorescence and CBB-stained gel image of MBP-^{E166N}TEM mixed with HEK293T cell lysate after incubation with CCD.

Scheme 1. Mechanism of β-Lactam Cleavage by Class A β-Lactamases; (E) Enzyme, (S) Substrate, and (P) Product

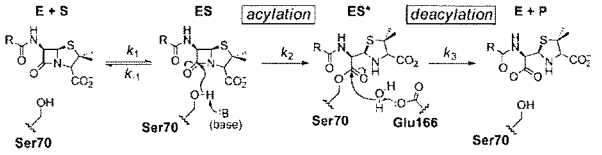

Scheme 2. Structures and Labeling Mechanisms of the Fluorescent Probes (a) CA and (b) CCD

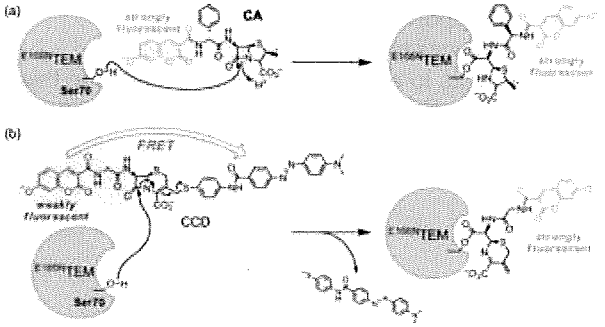

To investigate the feasibility of fluorescently labeling ^{E166N}TEM under physiological conditions, we designed and synthesized a penicillin-based fluorescent probe, coumarinyl ampicillin (CA). The labeling scheme is illustrated in Scheme 2a. Since CA contains 7-hydroxycoumarin, successfully labeled ^{E166N}TEM should exhibit cyan fluorescence. ^{E166N}TEM was incubated with CA in 10 mM Tris-HCl buffer (pH 7.0) at 25 °C, and protein labeling was assessed by SDS-PAGE. Fluorescent proteins were detected by irradiating the gels with UV light at 365 nm. When purified ^{E166N}TEM was mixed with CA, a protein band of ~29 kDa was observed that exhibited cyan fluorescence (Figure 1a); Coomassie Brilliant Blue (CBB) staining confirmed that this band corresponded to ^{E166N}TEM. In contrast, when wild-type (WT) TEM-1 was incubated with CA, no cyan fluorescence was seen (Figure S1a). Although CA successfully labels ^{E166N}TEM, other fluorescent bands were also observed on the gel. Since these bands were also seen when only

10.1021/ja8082285 CCC: $40.75

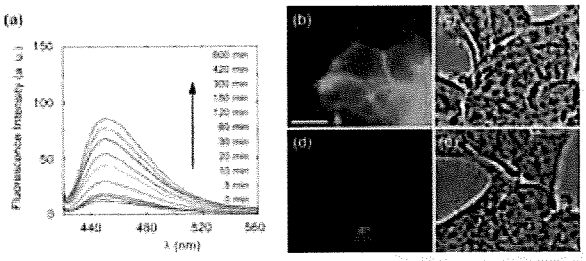

Figure 2. (a) Time-dependent emission spectra (λ_{ex} = 410 nm) of CCD (1 μM) in the presence of ^{E166N}TEM in 100 mM HEPES buffer (pH 7.4) containing 0.1% DMSO at 25 °C. (b–e) Optical microscopic images of CCD-labeled HEK293T cells expressing ^{E166N}TEM-EGFR (b,c) and EGFR (d,e), labeled with 5 μM CCD. (b,d) Fluorescence microscopic images, excitation at 410 nm. (c,e) phase contrast microscopic images. Scale bar: 10 μm.

CA was electrophoresed (Figure S2), a washing procedure should be performed before observation under a fluorescence microscope.

Next, we designed and synthesized CCD (Scheme 2b), a fluorescence off–on labeling probe. This molecule has three main components: 7-hydroxycoumarin, cephalosporin, and 4-(4′-dimethylaminophenylazo)benzoic acid (DABCYL). Since the absorption spectrum of DABCYL substantially overlaps with the emission spectrum of 7-hydroxycoumarin, the fluorescence of CCD would be expected to be largely quenched by intramolecular FRET from coumarin to DABCYL. Based on related probes of β-lactamase activity,[10] cleavage of the β-lactam of CCD by ^{E166N}TEM should result in covalent attachment of the coumarin to the protein with concomitant release of the DABCYL moiety as shown in Scheme 2b. After loss of the DABCYL group, the cyan fluorescence of coumarin should be restored by cancelation of FRET.

The fluorescence spectrum of CCD confirmed that the coumarin fluorescence was almost completely quenched because of FRET. The fluorescence quantum yield of CCD was 0.006, which is much lower than that of CA (Φ = 0.40). When CCD was incubated with ^{E166N}TEM, the fluorescence increased considerably in a time-dependent manner (Figure 2a). This indicates that ^{E166N}TEM cleaved the β-lactam of CCD and eliminated the DABCYL group. When the DABCYL group was completely eliminated by WT TEM-1, the fluorescence signal increased approximately 30-fold. The apparent rate of reaction between CCD and ^{E166N}TEM was approximately 80-fold slower than that of the reaction between CCD and WT TEM-1 (Figure S3), probably because the mutation at E166 decreases the acylation rate (k_2) somewhat.[15]

CCD specifically labels ^{E166N}TEM, as demonstrated by incubation of the probe molecule with both ^{E166N}TEM and WT TEM-1 in 10 mM Tris-HCl buffer (pH 7.0) at 25 °C, followed by SDS-PAGE analysis. As shown in Figure 1b, only the band corresponding to ^{E166N}TEM exhibited cyan fluorescence; no fluorescence was associated with WT TEM-1 (Figure S1b). In contrast to CA, unreacted CCD yielded considerably weaker fluorescence on the gel. In MALDI-TOF MS analyses of the samples, the molecular mass peak for the protein–probe adduct was only detected when ^{E166N}TEM was incubated with CCD (Figure S4).

This system can therefore be used to label target proteins in a biological medium. For example, we fused ^{E166N}TEM to maltose binding protein (MBP, 42 kDa), mixed the purified MBP–^{E166N}TEM construct with HEK293T cell lysate, and incubated the mixture with CCD at 25 °C for 45 min. SDS-PAGE analysis revealed that fusion protein was efficiently and selectively labeled with the fluorogenic probe (Figure 1c).

Finally, we investigated specific labeling of target proteins displayed on the surface of living cells. ^{E166N}TEM was fused to the N-terminus of epidermal growth factor receptor (EGFR), a membrane associated protein, and the construct was produced in HEK293T cells. After treatment with CCD (see Supporting Information), the cells were examined under a fluorescence microscope. Only cells producing the ^{E166N}TEM-EGFR fusion protein emitted cyan fluorescence as a consequence of specific labeling by the probe (Figure 2b–e).

In conclusion, we have developed a novel protein labeling system that combines a genetically modified β-lactamase with low molecular weight fluorogenic β-lactam probes. Through appropriate probe design, we succeeded in labeling proteins with a sensitive fluorophore in vitro and on living cells. In principle, this system does not require washing procedures to remove the unreacted probes after labeling. Furthermore, since the ^{E166N}TEM tag protein is absent in mammalian cells, it can be used for the specific labeling of proteins in higher eukaryotes. We anticipate that this labeling system will find wide application in the field of life science.

Acknowledgment. We thank Dr. Shahriar Mobashery at the University of Notre Dame for kindly providing TEM-1 plasmid. We also thank Dr. Robert E. Campbell at Alberta University, Dr. Gregor Zlokarnik at Vertex Pharmaceuticals, and Dr. Donald Hivert at ETH Zürich for helpful discussions. S.W. acknowledges a Global COE Fellowship of Osaka University. This work was supported in part by MEXT of Japan.

Supporting Information Available: Detailed experimental procedures and supplementary figures. This material is available free of charge via the Internet at http://pubs.acs.org.

References

(1) Chudakov, D. M.; Lukyanov, S.; Lukyanov, K. A. *Trends Biotechnol.* **2005**, *23*, 605–613.
(2) Griffin, B. A.; Adams, S. R.; Tsien, R. Y. *Science* **1998**, *281*, 269–272.
(3) Los, G. V.; et al. *ACS Chem. Biol.* **2008**, *3*, 373–382.
(4) Keppler, A.; Gendreizig, S.; Pick, H.; Vogel, H.; Johnsson, K. *Nat. Biotechnol.* **2003**, *21*, 86–89.
(5) Chen, I.; Howarth, M.; Lin, W.; Ting, A. Y. *Nat. Methods* **2005**, *2*, 99–104.
(6) Lin, C.-W.; Ting, A. Y. *J. Am. Chem. Soc.* **2006**, *128*, 4542–4543.
(7) Hauser, C. T.; Tsien, R. Y. *Proc. Natl. Acad. Sci. U.S.A.* **2007**, *104*, 3693–3697.
(8) Ojida, A.; Honda, K.; Shinmi, D.; Kiyonaka, S.; Mori, Y.; Hamachi, I. *J. Am. Chem. Soc.* **2006**, *128*, 10452–10459.
(9) Waley, S. G. *In the chemistry of β-lactams*; Page, M. I., Ed.; Chapman & Hall: London, 1992; p 198.
(10) (a) Moore, J. T.; Davis, S. T.; Dev, I. K. *Anal. Biochem.* **1997**, *247*, 203–209. (b) Zlokarnik, G.; Negulescu, P. A.; Knapp, T. E.; Mere, L.; Burres, N.; Feng, L.; Whitney, M.; Roemer, K.; Tsien, R. Y. *Science* **1998**, *279*, 84–88. (c) Gao, W.; Xing, B.; Tsien, R. Y.; Rao, J. *J. Am. Chem. Soc.* **2003**, *125*, 11146–11147. (d) Campbell, R. E. *Trends Biotechnol.* **2004**, *22*, 208–211. (e) Xing, B.; Khanamiryan, A.; Rao, J. *J. Am. Chem. Soc.* **2005**, *127*, 4158–4159.
(11) Sutcliffe, J. G. *Proc. Natl. Acad. Sci. U.S.A.* **1978**, *75*, 3737–3741.
(12) Matagne, A.; Lamotte-Blasseur, J.; Frére, J.-M. *Biochem. J.* **1998**, *330*, 581–598.
(13) Guillaume, G.; Vanhove, M.; Lamotte-Brasseur, J.; Ledent, P.; Jamin, M.; Joris, B.; Frére, J.-M. *J. Biol. Chem.* **1997**, *272*, 5438–5444.
(14) Adachi, H.; Ohta, T.; Matsuzawa, H. *J. Biol. Chem.* **1991**, *266*, 3186–3191.
(15) Vijayakumar, S.; Ravishanker, G.; Pratt, R. F.; Beveridge, D. L. *J. Am. Chem. Soc.* **1995**, *117*, 1722–1730.

JA8082285

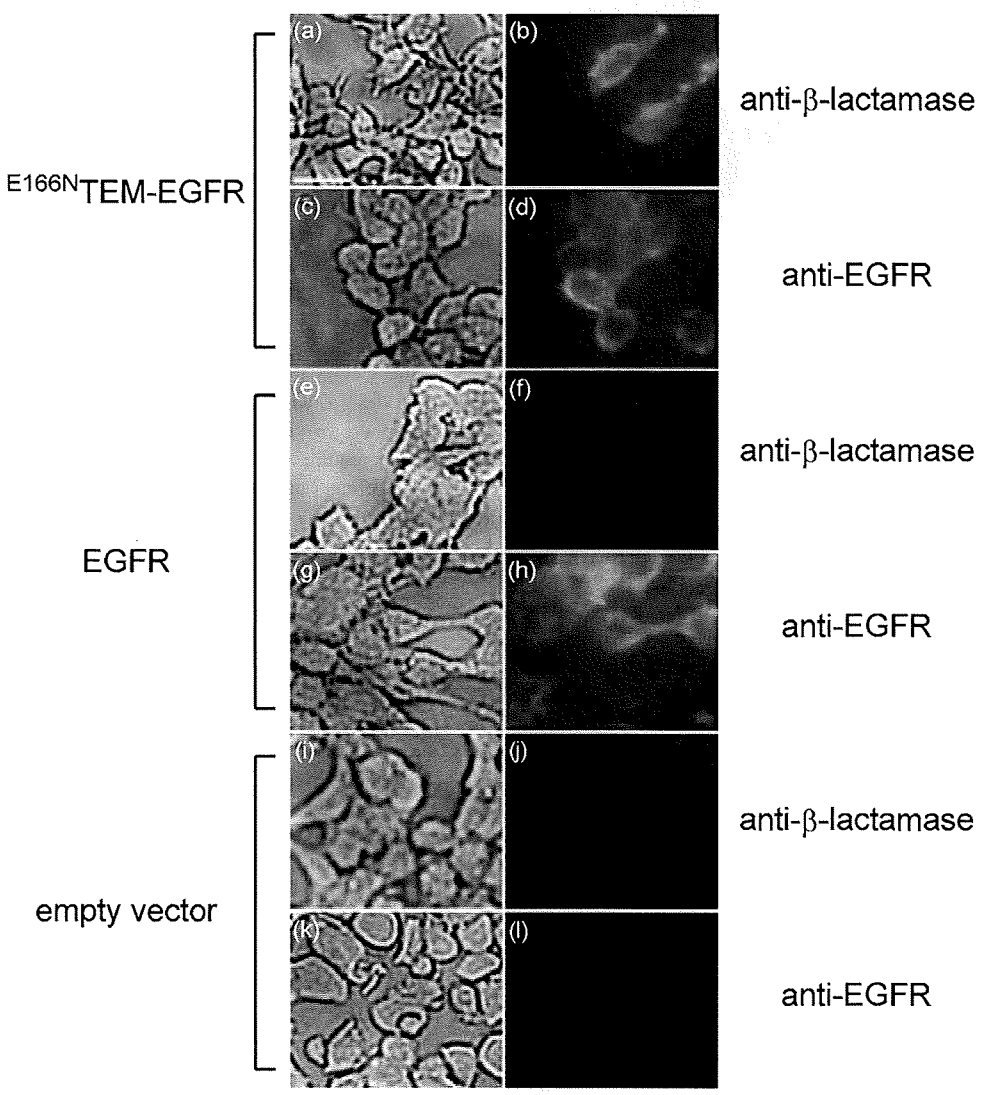

Figure S5. Optical microscopic images of HEK293T cells expressing (a–d) ^{E166N}TEM-EGFR, (e–h) EGFR, and (i–l) transfected with the empty vector, which were immunostained with the primary antibody ((b,f,j) anti-β-lactamase or (d,h,l) anti-EGFR) and the fluorescein-conjugated secondary antibody (scale bar: 20 μm). (b,d,f,h,j,l) Fluorescence microscopic images, excitation at 465 nm. (a,c,e,g,i,k) Phase contrast microscopic images.

DOI: 10.1002/anie.200806328

Molecular Imaging

Dual-Function Probe to Detect Protease Activity for Fluorescence Measurement and ^{19}F MRI**

*Shin Mizukami, Rika Takikawa, Fuminori Sugihara, Masahiro Shirakawa, and Kazuya Kikuchi**

Noninvasive molecular imaging techniques are important for understanding the actual mechanisms of biological systems. In biological sciences, especially those involving cellular systems, the most widely used imaging technique is fluorescence microscopy, because of its high sensitivity, high spatiotemporal resolution, and simple experimental procedure.[1] On the other hand, magnetic resonance imaging (MRI) is one of the most successful imaging techniques in the field of clinical diagnosis. As MRI can visualize deep regions of animal bodies,[2] application of MRI to in vivo imaging of biomolecules is attracting attention.[3] Several ^{1}H MRI probes have been developed to investigate pH values,[4] metal ions,[5] and enzyme activities.[6]

Recently, heteronuclear MRI has been attracting considerable attention as an alternative molecular imaging technique. One of the most promising nuclides for MRI is ^{19}F,[7] which has a high NMR sensitivity that is comparable to that of ^{1}H, and almost no intrinsic ^{19}F signals can be observed in living animals. ^{19}F MRI does not have the drawback of background signals from intrinsic biomolecules, which interfere with the probe signals. Very recently, we developed a novel design strategy for ^{19}F MRI probes that can detect protease activity.[8] We exploited the paramagnetic relaxation enhancement (PRE) effect to achieve off/on switching of the probe MRI signals (Scheme 1a). Using the ^{19}F MRI probe Gd-DOTA-DEVD-Tfb (Tfb = *para*-trifluoromethoxybenzyl) based on this mechanism, we were successful in detecting caspase-3 activity by ^{19}F MRI.

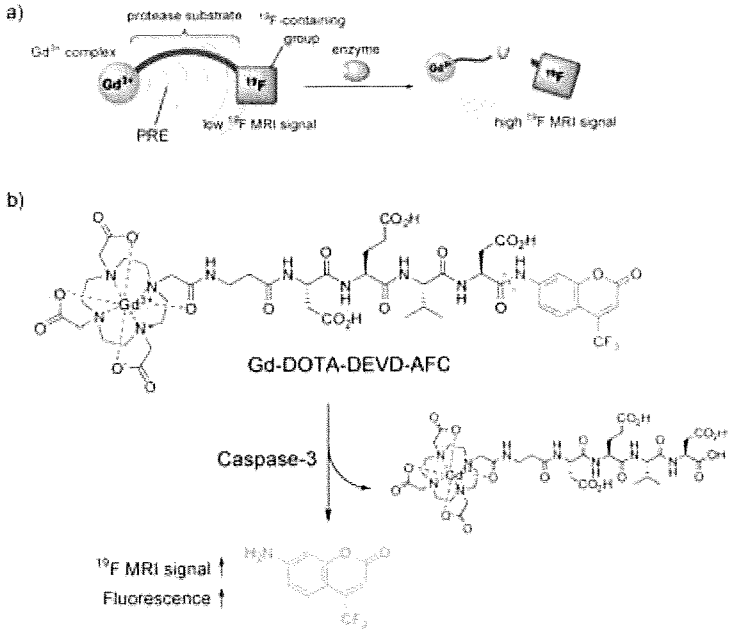

Scheme 1. a) Representation of ^{19}F MRI detection of protease activity. b) Chemical structure of Gd-DOTA-DEVD-AFC and its reaction scheme for detecting caspase-3 activity.

Although MRI can visualize deep regions of living bodies, its sensitivity is inferior to that of fluorescence measurement. The lower sensitivity requires longer accumulation time for imaging. If the probes are multifunctional, we can choose the appropriate imaging method in accordance with the experimental conditions. Higuchi et al. developed the dual-function probe (*E*,*E*)-1-fluoro-2,5-bis(3-hydroxycarbonyl-4-hydroxy)-styrylbenzene (FSB), which aggregates to amyloidβ (Aβ) plaques, for ^{19}F MRI and fluorescence measurements.[9] ^{19}F MRI signals localized on Aβ plaques were observed in living mice in vivo, and fluorescence signals in brain slices ex vivo.[9] As such complementary experiments have resulted in more reliable conclusions, development of multimodal imaging probes is very important.[10] Herein we report a dual-function probe to detect protease activity by fluorescence measurement and ^{19}F MRI that is based on the development of Gd-DOTA-DEVD-Tfb.[8]

We chose 7-amino-4-trifluoromethylcoumarin (AFC) as a reporter group that is active in both ^{19}F MRI and fluorescence measurement. AFC is strongly fluorescent in polar solvents,

[*] Dr. S. Mizukami, R. Takikawa, Prof. K. Kikuchi
Graduate School of Engineering
Osaka University, Osaka 565-0871 (Japan)
Fax: (+81) 6-6879-7924
E-mail: kkikuchi@mls.eng.osaka-u.ac.jp
Homepage: http://www-molpro.mls.eng.osaka-u.ac.jp/
F. Sugihara
International Graduate School of Arts and Sciences
Yokohama City University, Kanagawa 230-0045 (Japan)
Cellular & Molecular Biology Laboratory
RIKEN Advanced Science Institute
Saitama 351-0198 (Japan)
Prof. M. Shirakawa
Graduate School of Engineering
Kyoto University, Kyoto 615-8510 (Japan)
CREST, Science and Technology Corporation, Saitama 332-0012 (Japan)

[**] This work was supported in part by MEXT of Japan. MRI = magnetic resonance imaging.

Supporting information for this article is available on the WWW under http://dx.doi.org/10.1002/anie.200806328.

and the fluorescence properties of 7-aminocoumarin derivatives depend on the electron-donating ability of the 7-amino group.[11] Usually, the peptide modification on the 7-amino group induces a blue shift of the fluorescence spectrum with a decrease in fluorescence intensity. Thus, AFC has been utilized as the fluorophore for protease activity detection.[12] Furthermore, the ^{19}F NMR spectrum of AFC shows only a singlet peak without any coupling to intramolecular protons. AFC is thus appropriate for ^{19}F MRI.

We designed a bimodal probe Gd-DOTA-DEVD-AFC (Scheme 1), in which the probe consists of mainly three parts: Gd^{3+}-DOTA complex (DOTA = 1,4,7,10- tetraazacyclododecane-1,4,7,10-tetraacetate), caspase-3 substrate peptide (DEVD), and ^{19}F-containing fluorophore (AFC). When caspase-3 cleaves the C terminus of the DEVD sequence, AFC is produced. After the enzyme is cleaved, the ^{19}F MRI signal is increased in much the same manner as in Gd-DOTA-DEVD-Tfb (Scheme 1a). Simultaneously, the fluorescence spectrum of AFC is increased. Thus, Gd-DOTA-DEVD-AFC is expected to work as a bimodal probe that detects caspase-3 activity.

The Gd-DOTA-DEVD-AFC probe was synthesized using Fmoc solid-phase chemistry, followed by complex formation with the Gd^{3+} ion (Scheme 2). The excitation peak of Gd-DOTA-DEVD-AFC is at 340 nm, and irradiation at 400 nm results in little fluorescence emission. The incubation of the probe with caspase-3 at 37 °C induced the excitation spectral shift toward longer wavelengths. Therefore, when the probe was excited at 400 nm, the emission at around 500 nm was substantially increased (Figure 1). From the fluorescence measurements, the kinetic parameters for hydrolysis of Gd-DOTA-DEVD-AFC by caspase-3 were measured. The V_{max}/K_m value of Gd-DOTA-DEVD-AFC is $7.61 \times 10^{-3}\ s^{-1}$. On the other hand, V_{max}/K_m of Ac-DEVD-AMC, the commercially available fluorescent substrate (AMC = 7-amino-4-methylcoumarin), is $9.91 \times 10^{-4}\ s^{-1}$. This result indicates that Gd-DOTA complex does not hinder the enzyme reaction at all. Thus, Gd-DOTA-DEVD-AFC can be used as a superior fluorogenic probe for detecting caspase-3 activity.

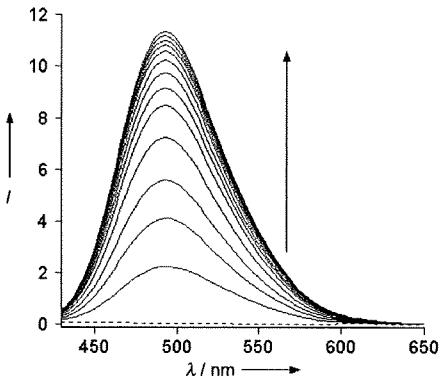

Figure 1. Time-dependent emission spectra of Gd-DOTA-DEVD-AFC (10 μM) with casapse-3 (0.84 mU) in the reaction buffer (pH 7.4) at 37 °C. The spectra were measured every 2 min after the addition of the enzyme. The dotted line indicates no caspase-3. The excitation wavelength: 400 nm. Reaction buffer: 4-(2-hydroxyethyl)-1-piperazineethanesulfonic acid (HEPES, pH 7.4, 50 mM) containing glycerol (10%), NaCl (100 mM), dithiothritol (DTT, 10 mM), ethylenediaminetetraacetic acid (EDTA, 1 mM), and 3-[(3-cholamidopropyl)dimethylammonio]-1-propanesulfonate (CHAPS, 0.1%).

We measured the ^{19}F NMR spectra of Gd-DOTA-DEVD-AFC and its metal-free analogue DOTA-DEVD-AFC. The NMR signal of Gd-DOTA-DEVD-AFC was broad and weak compared to that of the Gd^{3+}-free DOTA-DEVD-AFC (Supporting Information). This change in peak shape and intensity suggests that ^{19}F undergoes an intramolecular PRE effect from the Gd^{3+} ion. Longitudinal (T_1) and transverse (T_2) relaxation times of DOTA-DEVD-AFC (250 μM) were (0.479 ± 0.003) s and (0.152 ± 0.006) s, respectively (Table 1). In case of Gd-DOTA-DEVD-AFC, we could not estimate either T_1 or T_2, because these relaxation times were markedly shorter and the ^{19}F NMR signal intensity was low. From molecular modeling, the distance between the Gd^{3+} ion and the ^{19}F atom in the probe was estimated to be less than 25 Å. However, as the substrate peptide is flexible, the Gd^{3+} ion can be distributed in closer proximity to ^{19}F, such that the PRE effect works efficiently.

Next, we performed an enzyme assay using ^{19}F NMR spectroscopy. When Gd-DOTA-DEVD-AFC was treated with caspase-3 in the reaction buffer at 37 °C, a sharper and a more intense ^{19}F NMR signal was observed, with a slight downfield shift (Figure 2). T_1 and T_2 of the cleaved product (250 μM) were elongated to (0.38 ± 0.04) s and (0.097 ± 0.004) s, respectively (Table 1). This finding indicates that the intramolecular PRE effect from the Gd^{3+} ion to the ^{19}F atom was cancelled owing to the cleavage of the probe. After complete cleavage by

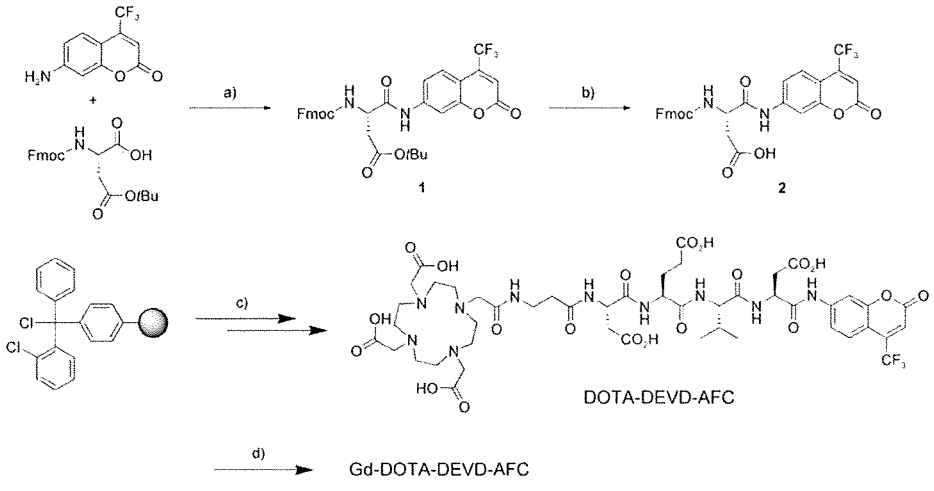

Scheme 2. Synthetic route to Gd-DOTA-DEVD-AFC. a) $POCl_3$, pyridine. b) trifluoroacetic acid. c) Fmoc peptide synthesis: **2**, Fmoc-Val-OH, Fmoc-Glu(OtBu)-OH, Fmoc-Asp(OtBu)-OH, Fmoc-β-Ala-OH, tris-tBu-DOTA, deprotection. d) $GdCl_3 \cdot 6H_2O$, 100 mM HEPES buffer (pH 7.4). Fmoc = fluorenylmethyloxycarbonyl.

Table 1: Longitudinal and transverse relaxation times of synthesized probes.

	T_1 [s][a]	T_2 [s][a]
DOTA-DEVD-AFC	0.479(3)	0.152(6)
Gd-DOTA-DEVD-AFC	_[b]	_[b]
Gd-DOTA-DEVD-AFC + caspase-3	0.38(4)[c]	0.097(4)[c]

[a] Parenthesis denotes standard deviation ($n=3$). [b] The relaxation time was too short to be determined. [c] The relaxation times were measured after the enzyme (250 μM) reaction was complete.

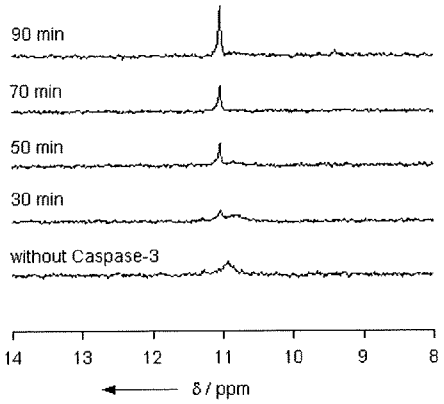

Figure 2. Time-dependent ^{19}F NMR spectra of Gd-DOTA-DEVD-AFC (250 μM) after addition of caspase-3 (1.25 mU) at 37 °C. Reaction buffer: As in Figure 1 plus D_2O (5%).

caspase-3 (confirmed by HPLC), the relaxation times T_1 and T_2 were lower than those observed for the metal-free ligand. These shorter relaxation times are most likely due to the intermolecular PRE of the cleaved Gd-DOTA (Supporting Information, Figure S4).

Finally, we attempted to visualize caspase-3 activity using a ^{19}F MRI phantom with Gd-DOTA-DEVD-AFC. Because of the extremely short relaxation time T_2, the ^{19}F MRI of Gd-DOTA-DEVD-AFC had no signals. When caspase-3 was added to the solution of Gd-DOTA-DEVD-AFC, augmentation of the ^{19}F MRI signal of the probe was observed (Figure 3).

In conclusion, we developed a novel dual-function probe, Gd-DOTA-DEVD-AFC, which detects caspase-3 activity by dual signal increase in fluorescence and in ^{19}F MRI. Because fluorescence measurement and MRI provide complementary information, such dual-mode probes should be quite useful for various biological experiments. Although several multimodal probes, such as fluorescence measurement and MRI, have been developed recently,[13] most probes are constructed by simple attachment of reporter moieties such as fluorescence dyes or MRI contrast agents. In contrast, multimodal probes accompanying plural signal enhancement have been scarcely reported. Such multimodal smart probes would be the next-generation probes in multimodal imaging for detecting enzyme activity.

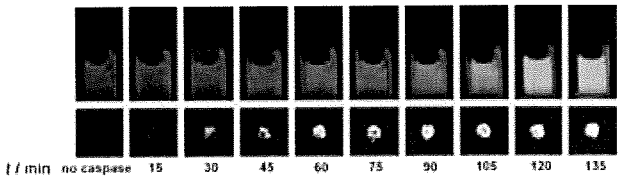

Figure 3. Time-dependent fluorescence images (top, λ_{ex}: 400 nm) and ^{19}F MR phantom images (bottom, diameter: approximately 2 mm) of Gd-DOTA-DEVD-AFC (10 μM for fluorescence measurement and 1 mM for ^{19}F MRI) with caspase-3 (60 nU for fluorescence measurement and 2 mU for ^{19}F MRI) at 37 °C. Reaction buffer: As in Figure 1. For ^{19}F MRI, [D_6]DMSO (20%) was introduced into the reaction buffer.

Received: December 26, 2008
Published online: April 7, 2009

Keywords: fluorescence · magnetic resonance imaging · molecular imaging · multimodal probe · proteases

[1] J. R. Lakovicz, *Principles of Fluorescence Spectroscopy*, 3rd ed., Springer Science & Business Media, New York, **2006**.
[2] a) A. Jasanoff, *Trends Neurosci.* **2005**, *28*, 120–126; b) D. E. Sosnovik, R. Weissleder, *Curr. Opin. Biotechnol.* **2007**, *18*, 4–10.
[3] R. Weissleder, M. J. Pittet, *Nature* **2008**, *452*, 580–589.
[4] a) S. Zhang, W. Kuangcong, A. D. Sherry, *Angew. Chem.* **1999**, *111*, 3382–3384; *Angew. Chem. Int. Ed.* **1999**, *38*, 3192–3194; b) S. Aime, A. Barge, D. D. Castelli, F. Fedeli, A. Mortillaro, F. U. Nielsen, E. Terreno, *Magn. Reson. Med.* **2002**, *47*, 639–648.
[5] a) W. Li, S. E. Fraser, T. J. Meade, *J. Am. Chem. Soc.* **1999**, *121*, 1413–1414; b) K. Hanaoka, K. Kikuchi, Y. Urano, M. Narazaki, T. Yokawa, S. Sakamoto, K. Yamaguchi, T. Nagano, *Chem. Biol.* **2002**, *9*, 1027–1032.
[6] a) A. Y. Louie, M. M. Hüber, E. T. Ahrens, U. Rothbächer, R. Moats, R. E. Jacobs, S. E. Fraser, T. J. Meade, *Nat. Biotechnol.* **2000**, *18*, 321–325; b) J. M. Perez, L. Josephson, T. O'Loughlin, D. Högemann, R. Weissleder, *Nat. Biotechnol.* **2002**, *20*, 816–820; c) B. Yoo, M. D. Pagel, *J. Am. Chem. Soc.* **2006**, *128*, 14032–14033; d) J. W. Chen, M. Q. Sans, A. Bogdanov, R. Weissleder, *Radiology* **2006**, *240*, 473–481.
[7] J. Yu, V. D. Kodibagkar, W. Cui, R. P. Mason, *Curr. Med. Chem.* **2005**, *12*, 819–848.
[8] S. Mizukami, R. Takikawa, F. Sugihara, Y. Hori, H. Tochio, M. Wälchli, M. Shirakawa, K. Kikuchi, *J. Am. Chem. Soc.* **2008**, *130*, 794–795.
[9] M. Higuchi, N. Iwata, Y. Matsuba, K. Sato, K. Sasamoto, T. C. Saido, *Nat. Neurosci.* **2005**, *8*, 527–533.
[10] a) E. A. Schellenberger, D. Sosnovik, R. Weissleder, L. Josephson, *Bioconjugate Chem.* **2004**, *15*, 1062–1067; b) Y. M. Huh, Y. W. Jun, H. T. Song, S. Kim, J. S. Choi, J. H. Lee, S. Yoon, K. S. Kim, J. S. Shin, J. S. Suh, J. Cheon, *J. Am. Chem. Soc.* **2005**, *127*, 12387–12391; c) P. Sharma, S. Brown, G. Walter, S. Santra, B. Moudgil, *Adv. Colloid Interface Sci.* **2006**, *123–126*, 471–485; d) J. H. Choi, F. T. Nguyen, P. W. Barone, D. A. Heller, A. E. Moll, D. Patel, S. A. Boppart, M. S. Strano, *Nano Lett.* **2007**, *7*, 861–867.
[11] C. E. Wheelock, *J. Am. Chem. Soc.* **1959**, *81*, 1348–1352.
[12] R. E. Smith, E. R. Bissel, A. R. Mitchell, K. W. Pearson, *Thromb. Res.* **1980**, *17*, 393–402.
[13] a) Y. M. Huh, Y. W. Jun, H. T. Song, S. Kim, J. S. Choi, J. H. Lee, S. Yoon, K. S. Kim, J. S. Shin, J. S. Suh, J. Cheon, *J. Am. Chem. Soc.* **2005**, *127*, 12387–12391; b) J. H. Lee, Y. W. Jun, S. I. Yeon, J. S. Shin, J. Cheon, *Angew. Chem.* **2006**, *118*, 8340–8342; *Angew. Chem. Int. Ed.* **2006**, *45*, 8160–8162; c) S. A. Corr, Y. P. Rakovich, Y. K. Gun'ko, *Nanoscale Res. Lett.* **2008**, *3*, 87–104; d) K. Tanaka, K. Inafuku, Y. Chujo, *Bioorg. Med. Chem.* **2008**, *16*, 10029–10033.

Zinc is an essential trace element for spermatogenesis

Sonoko Yamaguchi[a], Chiemi Miura[a], Kazuya Kikuchi[b], Fritzie T. Celino[a], Tetsuro Agusa[c,1], Shinsuke Tanabe[c], and Takeshi Miura[a,2]

[a]Research Group for Reproductive Physiology, South Ehime Fisheries Research Center, Ehime University, 1289-1, Funakoshi, Ainan, Ehime 798-4131, Japan; [b]Graduate School of Engineering, Osaka University, Osaka 565-0871, Japan; and [c]Center for Marine Environmental Science, Ehime University, Matsuyama 790-8577, Japan

Edited by Ryuzo Yanagimachi, University of Hawaii, Honolulu, HI, and approved May 8, 2009 (received for review January 19, 2009)

Zinc (Zn) plays important roles in various biological activities but there is little available information regarding its functions in spermatogenesis. In our current study, we further examined the role of Zn during spermatogenesis in the Japanese eel (*Anguilla japonica*). Human CG (hCG) was injected into the animals to induce spermatogenesis, after which the concentration of Zn in the testis increased in tandem with the progression of spermatogenesis. Staining of testicular cells with a Zn-specific fluorescent probe revealed that Zn accumulates in germ cells, particularly in the mitochondria of spermatogonia and spermatozoa. Using an in vitro testicular organ culture system for the Japanese eel, production of a Zn deficiency by chelation with *N,N,N′,N′*-tetrakis (2-pyridylemethyl)ethylenediamine (TPEN) caused apoptosis of the germ cells. However, this cell death was rescued by the addition of Zn to the cultures. Furthermore, an induced deficiency of Zn by TPEN chelation was found to inhibit the germ cell proliferation induced by 11-ketotestosterone (KT), a fish specific androgen, 17α,20β-dihydroxy-4-pregnen-3-one (DHP), the initiator of meiosis in fish, and estradiol-17β (E2), an inducer of spermatogonial stem-cell renewal. We also investigated the effects of Zn deficiency on sperm motility and observed that TPEN treatment of eel sperm suppressed the rate and duration of their motility but that co-treatment with Zn blocked the effects of TPEN. Our present results thus suggest that Zn is an essential trace element for the maintenance of germ cells, the progression spermatogenesis, and the regulation of sperm motility.

apoptosis | germ cells | in vitro culture | Japanese eel | sperm motility

Zinc (Zn) is well known as an essential trace element for a variety of biological activities. In biological systems, Zn is present in protein-bound and ionic forms, and plays important roles in mediating the function and structure of proteins, and in maintaining physiological balance. In vertebrates, Zn accumulates in the testis at high levels which are comparable to those in liver and kidney (1). In epidemiological studies in human, the inhibition of spermatogenesis and sperm abnormalities have been observed in patients with Crohn's disease and nutritional disorders, both of which induce a Zn deficiency (1–3). In vivo experiments in rodents have also demonstrated that a Zn deficiency can cause severe damage to the testes such as atrophy of the testicular tubules and the inhibition of spermatid differentiation (4, 5). Moreover, there are some reports that exposure to Zn can alleviate testis damage by stresses such as heavy metals, fluoride, and heat (6). These findings suggest that the testes may harbor a Zn-incorporation system, and that Zn itself may exert protective effect against testicular injury and play an essential role in the maintenance of testicular functions. However, there has been no evidence reported to date that shows any direct effects of Zn upon spermatogenesis in vertebrates.

In contrast to spermatogenesis, the effects of Zn on sperm motility have been examined in a number of vertebrate and invertebrate species. In humans, sperm motility declines in association with increased Zn concentrations in the seminal plasma (7). Morisawa and Yoshida have also reported that Zn in the seminal plasma of human suppresses sperm motility, and that the removal of Zn by binding to a protein named semenogelin enhances motility (6). On the other hand, in sea urchin, treatment with the bivalent metal ion chelator, ethylenediamine tetra acetic acid (EDTA), inhibits sperm motility that is reversed by the addition of Zn (9). These results suggest that extracellular Zn indeed affects sperm motility but whether this is inhibitory or stimulatory appears to be species-specific. Additionally, it has been reported that Zn is present in sperm mitochondria and flagella (10, 11) but there had been no reports to date concerning the role of intracellular Zn upon sperm function.

To further study the role of Zn upon spermatogenesis in our current study, we chose Japanese eel (*Anguilla japonica*) as our animal model. In the Japanese eel in vivo, a complete pathway of spermatogenesis, from the spermatogonia stage to sperm maturation, can be induced by the injection of human CG (hCG; 12). Furthermore, we have developed a testicular organ culture system for the Japanese eel in our laboratory, which is the only currently available system of its kind in which the induction of complete spermatogenesis can be performed in vitro by the addition of 11-ketotestosterone or hCG (13, 14). By in vivo and in vitro analyses of spermatogenesis in the Japanese eel, we have previously further clarified the regulatory mechanisms underlying fish spermatogenesis (15, 16). Additionally, we have revealed the inhibitory effects of 4 trace elements (lead, molybdenum, rubidium, and arsenic) on fish spermatogenesis using our in vitro testicular organ culture system (17). In our present study, we again used the Japanese eel model to investigate the concentration and distribution of Zn in testis during spermatogenesis. Moreover we examined the effects of Zn addition and deficiency on spermatogenesis and sperm motility in vitro.

Results

Changes in the Levels and Distribution of Zinc (Zn) in the Testis of the Japanese Eel during Spermatogenesis. Before injection with hCG, the concentration of Zn in the testis of the Japanese eel was approximately 50 μg/g. After injection, the Zn concentration in the testis gradually increased, and the highest levels were observed on day 9. Thereafter, the concentration of Zn remained at high levels until day 18 (Fig. 1).

To detect the distribution of Zn in eel testes, an unfixed testicular fragment was stained with a fluorescence sensor for Zn(II), ZnAF-2DA. Strong fluorescent signals were obtained in the lobules but not in the interstitial tissue (Fig. 2*A* and *B*). We thus further investigated the distribution of Zn in testicular tissue using isolated cells. Germ cells were found to be strongly stained

Author contributions: S.Y., C.M., and T.M. designed research; S.Y., C.M., F.T.C., T.A., S.T., and T.M. performed research; K.K. contributed new reagents/analytic tools; S.Y., C.M., and T.M. analyzed data; and S.Y., C.M., and T.M. wrote the paper.

The authors declare no conflict of interest.

This article is a PNAS Direct Submission.

[1]Present address: Faculty of Medicine, Shimane University, Izumo, Shimane 693-8501, Japan.

[2]To whom correspondence should be addressed. E-mail: miutake@agr.ehime-u.ac.jp.

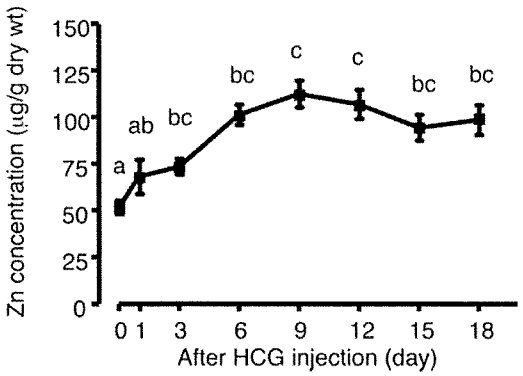

Fig. 1. Changes in the Zn concentrations in the testis of the Japanese eel after injection of human CG (hCG). The different letters indicate statistically significant differences ($P < 0.05$).

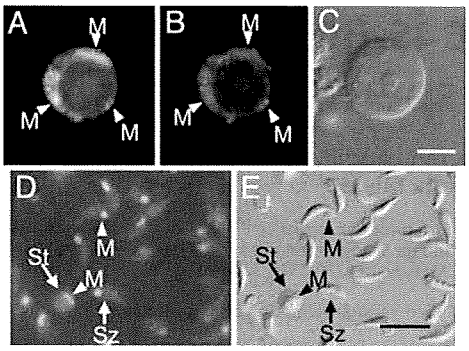

Fig. 3. Zinc distribution in germ cells of the Japanese eel. Zn was stained using ZnAF-2DA. Fluorescence images are shown for (*A*) Zn, and (*B*) mitochondria. (*C*) Bright field image of spermatogonia. (*D*) Zn fluorescence and (*E*) bright field image of spermatids and spermatozoa. M, mitochondria; St, spermatid; Sz, spermatozoa. (Scale bars: 10 μm.)

by ZnAF-2DA but Sertoli cells showed no signal (Fig. 2 *C* and *D*). When the germ cells were treated with 10 mM *N,N,N′,N′*-tetrakis(2-pyridylemethyl) ethylenediamine (TPEN) for 1 h before staining with ZnAF-2DA, fluorescence was not detected (Fig. 2 *E* and *F*). We also stained the germ cells at various stages with ZnAF-2DA, that is, spermatogonia, spermatocytes, spermatids, and spermatozoa. ZnAF-2DA signals were detectable in spermatogonia, most notably in the mitochondria (Fig. 3 *A–C*). Additionally, the mitochondria of the spermatids and spermatozoa also displayed strong ZnAF-2DA signals (Fig. 3 *D* and *E*).

Effects of Zn and Zn Chelators on Japanese Eel Testes in Vitro. To investigate the putative key role of Zn during spermatogenesis, we analyzed the direct effects of Zn on the testis in the presence or absence of 11-ketotestosterone (KT). After culturing for 6 days, testicular fragments in the control group were found to be occupied by type A spermatogonia. Although the histological structure of the testicular fragments cultured with KT alone did not differ from the control group, the incorporation ratio of BrdU into the germ cells had significantly increased (Fig. 4), as also reported in our previous study (13). Treatment of the Japanese eel testicular fragments with any level of Zn with or without KT did not affect the histology of the testis or the BrdU index (Fig. 4*A*). Treatment with ethylenediamine-*N,N,N′,N′*-tetraacetic acid, calcium(II), disodium salt (Ca-EDTA), an extracellular Zn chelator, also did not affect the BrdU index or testicular morphology after 6 days in culture (Figs. 4*B* and 5*B*). In contrast, exposure to 0.01 and 0.1 mM TPEN, an intracellular chelator of Zn, inhibited BrdU-incorporation into germ cells (Fig. 4*B*), and induced germ cell death (Figs. 4*B* and 5*C*). Significantly, both the cell death and the inhibition of BrdU incorporation induced by TPEN was rescued by the addition of Zn (Figs. 4*B* and 5*D*). We further investigated the type of cell death that occurred using a TdT-mediated dUTP nick-end

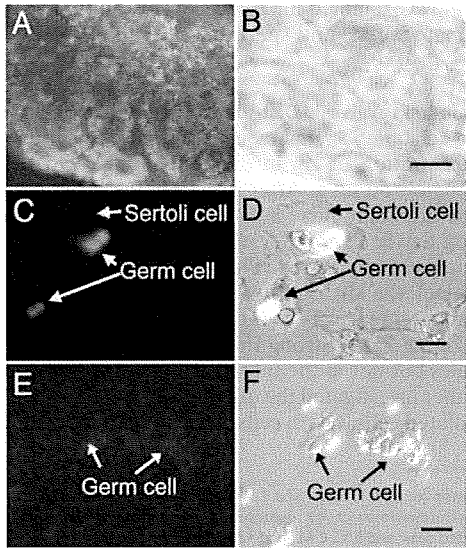

Fig. 2. The zinc distribution in the testis of the Japanese eel determined by staining with a Zn-specific fluorescent probe, ZnAF-2DA (*A*, *C*, and *E*). Bright field images are also shown (*B*, *D*, and *F*). (*A* and *B*) testicular fragments of the Japanese eel at 15 days after injection of hCG; (*C* and *D*) germ cells and Sertoli cells; (*E* and *F*) TPEN-treated germ cells. (Scale bars: *A* and *B*, 100 μm; *C–F*, 20 μm.)

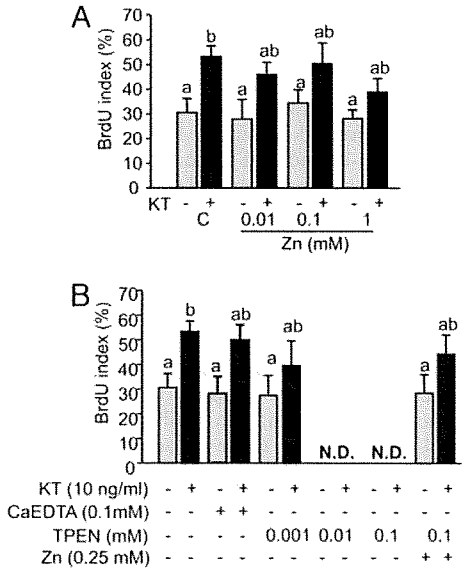

Fig. 4. Effects of Zn and Zn chelators on the early stages of spermatogenesis in vitro. The BrdU-labeling index was determined for germ cells in testicular fragments cultured with Zn (*A*) or Zn chelators (*B*) with or without KT. The number of BrdU-positive germ cells is expressed as a percentage of the total number of germ cells. C, control; Zn, $ZnCl_2$; KT, 11- ketotestosterone; TPEN, *N,N,N′,N′*-tetrakis(2-pyridylmethyl)ethylenediamine; CaEDTA, ethylenediamine -*N,N,N′,N′*- tetraacetic acid, calcium(II), disodium salt, dihydrate. Results are given as the mean ± SEM. The different letters on the columns indicate statistically significant differences ($P < 0.05$).

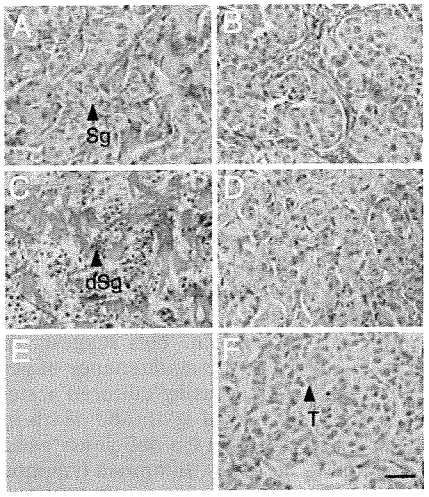

Fig. 5. Light micrographs of testicular fragments after culture with Zn chelators for 6 days. (*A–D*) Hematoxylin and eosin-stained testicular fragments cultured for 6 days. (*A*) control; (*B*) cultured with 0.1 mM CaEDTA; (*C*) cultured with 0.01 mM TPEN; (*D*) cultured with 0.1 mM TPEN and 0.25 mM $ZnCl_2$. (*E* and *F*) One-day cultures of testicular fragments subjected to a TUNEL assay. (*E*) control; (*F*) cultured with TPEN. Dark stained cells are TUNEL-positive (*E* and *F*). Sg, spermatogonia; dSg, dead spermatogonia; T, TUNEL-positive cells. (Scale bar: 20 μm.)

labeling (TUNEL) assay after a 1-day culture in the presence of TPEN. In the control and KT-treatment groups, no cell staining was observed (Fig. 5*E*). However, TUNEL-positive germ cells were detectable after treatment with 0.01–0.1 mM TPEN with or without KT (Fig. 5*F*).

We also investigated the effects of 0.001 mM TPEN, a dose that does not cause cell death, upon KT-induced spermatogenesis using our testicular organ culture system. Treatment with this dosage for 6 days had no effects on the histological structure of the testicular fragments. In contrast, after 15 days of this treatment, the testicular fragments were found to only have type A spermatogonia, although those cultured with KT alone contained the more progressed germ cells, type B spermatogonia (Fig. 6 *A–C*). Importantly, the addition of Zn led to a recovery of spermatogenesis, such that the TPEN/KT treated cultures resembled those exposed to KT alone (Fig. 6*D*).

Effects of Zn on the Germ Cell Proliferation Induced by Various Steroid Hormones. In the Japanese eel, KT, 17α,20β-dihydroxy-4-pregnen-3-one (DHP), and estradiol-17β (E2) induce DNA

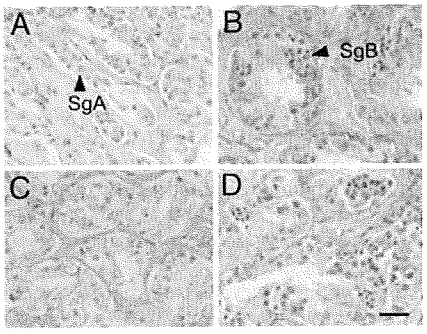

Fig. 6. Light micrographs of testicular fragments after culture with 10 ng/mL KT and 0.001 mM TPEN for 15 days. (*A*) Control; (*B*) cultured with 10 ng/mL KT; (*C*) cultured with KT and 0.001 mM TPEN; (*D*) cultured with KT, TPEN, and 0.0025 mM $ZnCl_2$. SgA, type A- spermatogonia; SgB, type B-spermatogonia. (Scale bar: 20 μm.)

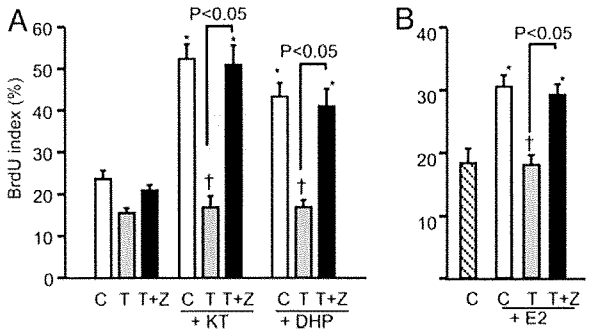

Fig. 7. Effects of a low dose TPEN upon germ cell proliferation in vitro. Testicular fragments were cultured with 0.001 mM TPEN and/or 10 ng/mL KT or DHP for 6 days (*A*) or cultured with TPEN and/or 1 ng/mL E2 (*B*). (*C*) Testicular fragments cultured without TPEN as a control for each steroid hormone; T, with TPEN; T+Z, with TPEN and Zn. KT, 10 ng/mL 11- ketotestosterone; DHP, 10 ng/mL 17α,20β-dihydroxy-4-pregnen-3-one; E2, 1 ng/mL estradiol-17β. Asterisks indicate significant differences from the negative control ($P < 0.05$). Daggers indicate significant differences from the control for each steroid hormone treatment ($P < 0.05$).

synthesis in germ cells thereby initiating spermatogenesis, meiosis, and spermatogonial stem-cell renewal, respectively (13, 16, 18). To elucidate at the stages of spermatogenesis at which Zn functions, that is, spermatogonial stem-cell renewal, spermatogonial proliferation or meiosis, we examined the effects of a 0.001 mM concentration of an intracellular Zn chelator on the germ cell proliferation induced by 10 ng/mL KT, 1 ng/mL E2, and 10 ng/mL DHP. These doses of KT, DHP and E2 were previously shown to be optimal for the induction of DNA synthesis in germ cells in vitro involving the initiation of spermatogenesis, meiosis, and spermatogonial stem-cell renewal, respectively (13, 16, 18). The rates of BrdU incorporation increased after treatment with KT and DHP for 6 days. However, treatment with 0.001 mM TPEN decreased the levels of BrdU incorporation induced by DHP or KT (Fig. 7*A*). To then investigate the effects of Zn on E2-induced germ cell proliferation, eel testes were cultured with E2 with or without 0.001 mM TPEN for 15 days according to the method of Miura et al. (18). Treatment with E2 alone significantly increased the number of BrdU-positive germ cells, whereas E2 in combination with 0.001 mM TPEN suppressed germ cell proliferation. This inhibition by TPEN was rescued by Zn treatment (Fig. 7*B*).

Effects of Zn Deficiency on Sperm Motility. In the mitochondria of Japanese eel sperm, strong ZnAF-2DA signals were observed. Hence, we analyzed the effects of Zn chelators on the rate and duration of eel sperm motility. Treatment of the sperm with Ca-EDTA did not alter their motility rate or duration at any concentration (Fig. 8*A* and *B*). In contrast, the addition of TPEN decreased both the motile rate and duration in a dose-dependent manner: 0.1–1 mM TPEN was found to be an effective concentration range for both indices. Furthermore, treatment with 1 mM Zn treatment rescued the inhibition of sperm motility by 1 mM TPEN (Fig. 8 *A* and *B*).

Discussion

Some previous studies have reported that a high concentration of Zn is detectable in testis, and that a Zn deficiency inhibits spermatogenesis and causes sperm abnormalities (5, 19). However, there are currently few reports that address the function of Zn during spermatogenesis in any detail. We thus investigated in our current study the distribution of Zn in testis and the direct effects of Zn upon spermatogenesis using an in vitro testicular organ culture model derived from the Japanese eel.

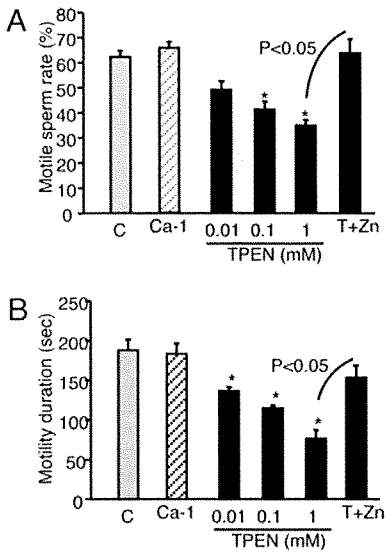

Fig. 8. Effects of Zn chelators on the motility of Japanese eel sperm. (*A*) Ratio of motile sperm; (*B*) duration of sperm motility. C, control; Ca-1, incubated with 1 mM Ca-EDTA; T+Z, incubated with 1 mM TPEN and 1 mM $ZnCl_2$. Asterisks indicate statistically significant differences from the control.

Our present analyses show that the Zn concentration in the testes of the Japanese eel gradually increases following an injection with hCG, and peaks on day 9 after this induction. Additionally, using a fluorescent Zn probe, strong signals were observed in germ cells, particularly spermatogonia, but not in the interstitial tissue or Sertoli cells. Similar to our present findings, Sørensen et al. have previously demonstrated by autometallography (AMG) that Zn is present in spermatogonia and primary spermatocytes in mouse (20). We previously demonstrated in our laboratory that a single injection of hCG first induced spermatogonial proliferation, then initiated meiosis on about day 12, and induced spermiogenesis on day 18 postinjection (12). Taken together therefore, our current data and previous findings suggest that Zn accumulates in the testis during early spermatogenesis, and may play a key role in the regulation of the spermatogonial proliferation and in the meiosis of germ cells. In the germ cells of other vertebrates, some Zn transporters have been observed. In rat, metallothionein (MT) was detected in spermatocytes (21) and other reports have shown that a testis-specific metallothionein-like protein (tesmin) is also present in these cells (22, 23). Additionally, Chi et al. have demonstrated that Zn accumulates in sperm in the mouse and that the Zn-exporter, ZnT-7, is present in the mouse testis, suggesting that Zn may be supplied to the germ cells via ZnT-7 (24). We speculate therefore that Zn may be accumulated in the germ cells of the Japanese eel via such transporter molecules.

In our present experiments in eel, Zn was found to accumulate prominently in the mitochondria in spermatogonia, spermatids and spermatozoa. In mouse, as detected via the AMG technique, sperm mitochondria were also previously shown to accumulate Zn, similar to our current results (10). Costello et al. have reported that Zn is imported into the mitochondria of prostate and liver cells in the form of a Zn-ligand complex such as Zn-citrate and Zn-MT (25, 26). Additionally, the membrane type Zn transporter protein ZnT-1 is expressed in the mitochondria of mouse spermatozoa (21). Taken together, there is now ample evidence to suggest that mitochondria may harbor a transporting system for Zn, and that Zn itself may have an important role to play in mitochondrial function in germ cells. In addition to mitochondria, Zn has also been detected in other areas of the cytoplasm in eel spermatogonia. In rat, Zn accumulates in the cytoplasm of both spermatogonia and spermatocytes (20). Furthermore, murine ZnT-7 is present in Golgi apparatus of spermacytes and spermatids (24). Thus, other organelles and cytosolic compartments may also accumulate Zn as part of its germ cell functions.

To further clarify the role of Zn in germ cells, we also investigated the effects of Zn and intra/extracellular Zn chelators on spermatogenesis using our in vitro testicular organ culture system develop from the Japanese eel. The results of these experiments demonstrated that treatment with the intracellular chelator TPEN caused germ cell death, which was blocked by the addition of Zn. This suggests that Zn is an essential trace element for the maintenance of germ cells. We performed a TUNEL assay using cultured testes and found that TPEN specifically caused apoptotic death in germ cells. There are some reports that a Zn deficiency causes apoptosis in various cell and tissue types. In human lymphocytes and rat hepatocytes for example, treatment with TPEN causes DNA fragmentation (27, 28). Interestingly, an in vitro and in vivo Zn deficiency was shown to induce caspase-3 activity in human mast cells and rat embryos, respectively (29, 30). Furthermore, treatment with Zn induces the antiapoptotic protein Bcl-2 and inhibits apoptosis in U947 cells (31). Caspase-3 and Bcl-2 in mitochondria have important roles in mitochondrial apoptosis; caspase-3 is released after cell damage and induces apoptosis, whilst Bcl-2 suppresses the apoptotic response (32). In our present study using a fluorescent Zn probe, we found that Zn accumulates in the mitochondria of germ cells and this may underpin its protection of these cells from apoptosis. However, the molecular mechanisms of how Zn regulates caspase-3 and Bcl-2 in mitochondria remain unclear at present. Some studies have addressed the correlation between Zn and apoptosis and suggest that Zn may function as an antioxidant in cells (32). Further studies will be necessary to clarify the role of Zn in the maintenance of germ cells.

We additionally investigated the influence of mild Zn deficiency on spermatogonial stem-cell renewal, spermatogonial proliferation, and meiosis in vitro. In a previous study, we reported that KT, E2, and DHP induce spermatogenesis, spermagonial stem-cell renewal, and meiosis in eel germ cells, respectively (13, 15, 16). In our present report, TPEN was found to inhibit all steroid hormone-induced DNA synthesis in the testes of the Japanese eel. These results suggest that Zn has an important role in DNA synthesis involving mitotic cell proliferation and meiosis. A previous study using 3T3 cells has reported that treatment with the Zn chelator, diethylenetriaminepentaacetic acid, decreases the mRNA expression and activity of thymidine kinase, after which DNA synthesis was inhibited in 3T3 cells (33). Furthermore, steroid hormone receptors such as progestin, androgen, and estrogen receptors all harbor Zn finger motifs within their structures (34). Other transcription factor genes containing Zn-finger motifs are also expressed during spermatogenesis (35). These findings suggest therefore that during steroid hormone-induced DNA synthesis, germ cells may incorporate Zn to activate a number of specific enzyme and Zn finger proteins, which are functionally disrupted by TPEN. Further analyses will be necessary to clarify the role of Zn on the functions of steroid hormone receptors and transcription factors during spermatogenesis.

Our current findings demonstrate that treatment with TPEN decreases sperm motility in the Japanese eel. Consistently in this regard, studies of human sperm have also demonstrated that diethyldithiocarbamate, which is an intracellular Zn chelator, inhibits sperm motility and decreases sperm velocity (36). These results suggest that intracellular Zn is important for sperm motility. As mentioned above, the mitochondria in the sperm of